

**NASA TECHNICAL
MEMORANDUM**

NASA TM X-73,215

NASA TM X-73,215

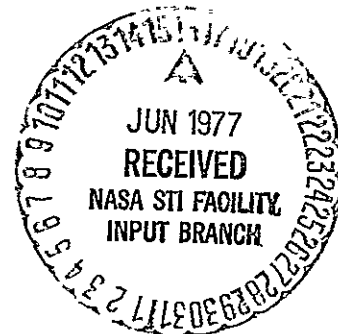
**INVESTIGATION OF INLET CONCEPTS FOR MANEUVER IMPROVEMENT
AT TRANSONIC SPEEDS**

(NASA-TM-X-73215)	INVESTIGATION OF INLET	N77-24060
CONCEPTS FOR MANEUVER IMPROVEMENT AT		
TRANSONIC SPEEDS (NASA)	61 p HC A04/MF A01	
	CSCCL 01A	Unclas
		G3/02 30346

By Eldon Latham, John Gawienowski and Frank Meriwether

Ames Research Center
Moffett Field, California 94035

April 1977



1. Report No. TM X-73,215		2. Government Accession No.		3. Recipient's Catalog No.	
4. Title and Subtitle INVESTIGATION OF INLET CONCEPTS FOR MANEUVER IMPROVEMENT AT TRANSONIC SPEEDS				5. Report Date April 1977	
				6. Performing Organization Code	
7. Author(s) Eldon Latham, John Gawienowski and Frank Meriwether				8. Performing Organization Report No. A-6952	
9. Performing Organization Name and Address NASA-Ames Research Center Moffett Field, Ca. 94035				10. Work Unit No. 505-04-11	
				11. Contract or Grant No.	
12. Sponsoring Agency Name and Address National Aeronautics and Space Administration Washington D.C. 20546				13. Type of Report and Period Covered Technical Memorandum	
				14. Sponsoring Agency Code	
15. Supplementary Notes					
16. Abstract A 15-percent-scale lightweight fighter-type inlet-forebody was tested in the Ames 14-Foot Transonic Wind Tunnel at Mach numbers of 0.7, 0.9, and 1.04. The inlet was a two-dimensional horizontal-ramp system designed for a Mach number of 2.2. Four inlet devices designed to prevent or delay cowl-lip boundary-layer separation or to improve the inlet internal flow characteristics at high angles of attack were investigated. The devices used to control cowl-lip separation consisted of cowl leading-edge flaps, slotted flaps, and tangential blowing. To improve the internal flow characteristics, discrete jet-nozzle flows were directed downstream and parallel to the duct surface in the subsonic diffuser to energize the wall boundary layer. The discrete jets used in the subsonic diffuser were also tested in combination with each of the cowl leading-edge devices. The Reynolds number was about 11.9×10^6 per meter (3.9×10^6 per foot) for all Mach numbers. Angle of attack ranged from 0° to 56° and angle of sideslip from 0° to 15° . Test measurements included engine-face total pressure recovery, steady state distortion, dynamic distortion, duct boundary-layer profiles, and duct-surface static pressures. This report includes only representative data of some of the important parameters. No dynamic data are included.					
17. Key Words (Suggested by Author(s)) Inlet Transonic Maneuver High Angle of Attack			18. Distribution Statement Unlimited STAR Category 02		
19. Security Classif. (of this report) Unclassified		20. Security Classif. (of this page) Unclassified		21. No. of Pages 59	22. Price* \$4.25

INVESTIGATION OF INLET CONCEPTS FOR
MANEUVER IMPROVEMENT AT TRANSONIC SPEEDS

By Eldon Latham, John Gawienowski and Frank Meriwether*

Ames Research Center

SUMMARY

A 15-percent-scale lightweight fighter-type inlet-forebody was tested in the Ames 14-foot Transonic Wind Tunnel at Mach numbers of 0.7, 0.9, and 1.04. The inlet was a two-dimensional horizontal-ramp system designed for a Mach number of 2.2. Four inlet devices designed to prevent or delay cowl-lip boundary-layer separation or to improve the inlet internal flow characteristics at high angles of attack were investigated. The devices used to control cowl-lip separation consisted of cowl leading-edge flaps, slotted flaps, and tangential blowing. To improve the internal flow characteristics, discrete jet-nozzle flows were directed downstream and parallel to the duct surface in the subsonic diffuser to energize the wall boundary layer. The discrete jets used in the subsonic diffuser were also tested in combination with each of the cowl leading-edge devices. The Reynolds number was about 11.9×10^6 per meter (3.9×10^6 per foot) for all Mach numbers. Angle of attack ranged from 0° to 56° and angle of sideslip from 0° to 15° . Test measurements included engine-face total pressure recovery, steady state distortion, dynamic distortion, duct boundary-layer profiles, and duct-surface static pressures. This report includes only representative data of some of the important parameters. No dynamic data are included.

INTRODUCTION

Aerodynamic design and control improvements have resulted in expanded stable-maneuver-envelopes for tactical aircraft. This type of aircraft requires advanced inlet concepts to provide good pressure recovery and low flow distortion to maintain continuous high thrust levels and prevent engine stall during severe maneuvers.

The purpose of this investigation was to evaluate the performance characteristics of selected inlet devices designed to prevent or delay cowl-lip boundary-layer separation or to control the inlet-duct flow properties so as to obtain maximum inlet pressure recovery and minimum flow distortion during severe transonic maneuvering. Four such devices were tested. Three

* Project Engineer, ARO, Inc., Moffett Field, Calif. 94035

of these devices were derived from wing leading-edge high-lift devices and consisted of cowl leading-edge flaps, slotted flaps, and tangential blowing. The fourth device consisted of discrete jet-nozzle flow directed downstream and parallel to the duct surface in the subsonic diffuser so as to energize the wall boundary-layer. This fourth device was also tested in combination with each of the cowl leading-edge devices.

The test program, which was a cooperative effort between NASA Ames and General Dynamics, Fort Worth Division, was conducted in the Ames 14-Foot Transonic Wind Tunnel at Mach numbers of 0.7, 0.9, and 1.04. Angle of attack ranged from 0° to 56° and angle of sideslip from 0° to 15°. The Reynolds number was essentially constant and equal to 11.9×10^6 per meter (3.9×10^6 per foot) for all Mach numbers. Test measurements included engine-face total-pressure recovery, steady state distortion, dynamic distortion, duct boundary-layer profiles and duct-surface static pressures.

NOMENCLATURE

<u>Symbol</u>	<u>Definition</u>
ALPHA, α	angle of attack of model reference axis, deg
(AN/NSGRPT)MAX	maximum normalized Fourier coefficient parameter for ring 1 through ring 5, respectively
AO/AI	capture area ratio
BETA, β	angle of sideslip of model reference axis, deg
CFabb	compressor face total pressure ratios, <u>compressor pressure</u> a = ring number, bb = rake number PT
CONF	configuration code number
CMUL	actual combined lip and diffuser blowing momentum coefficient
CMUO	theoretical combined lip and diffuser blowing momentum coefficient
CMUxL	actual isolated blowing momentum coefficient, x - 1 = cowl lip, 2 = diffuser
CMUx0	theoretical isolated blowing momentum coefficient, x - 1 = cowl lip, 2 = diffuser

<u>Symbol</u>	<u>Definition</u>
DS	splitter diameter, calculated size of high compressor region, 1
D2	maximum compressor distortion, $\frac{\text{max. CFabb} - \text{min CFabb}}{PT}$
DX1	normalized KA2
DX2	normalized KC2
FLAP/SLAT	angle of cowl lip flap or slat relative to model reference axis, positive downward, deg
GX1	prediction of instantaneous DX1
ID	engine/inlet stability index
IDCy	compressor circumferential distortion index, y = compressor total-pressure ring number
IDCHUB	hub circumferential distortion index, $\frac{IDC1 + IDC2}{2}$
IDCMAX	larger of IDCHUB and TIP
IDCTIP	tip circumferential distortion index, $\frac{IDC4 + IDC5}{2}$
IDRMAX	larger of IDR4 and IDR5
IDRy	compressor radial distortion index, y = compressor total pressure-ring number
KA2	combined circumferential and radial distortion index
KC2	high compressor distortion parameter
KRA2	fan radial distortion parameter
KTHETA	fan circumferential distortion parameter
KTHETAS	fan circumferential distortion for rings with diameter < DS
MACH, M	free-stream Mach number
MTH	inlet throat Mach number

<u>Symbol</u>	<u>Definition</u>
P	free-stream static pressure, psf
PA1	lip blowing plenum pressure, psia
PA2	diffuser blowing plenum pressure, psia
PDcdd	duct wall static pressure ratios, $\frac{\text{duct pressure}}{P_T}$ c - 1 = upper wall, 2 = lower wall dd = tap number
PDX	lip blowing static pressure, $\frac{(PD201) (P_T)}{144}$, psia
PDY	diffuser blowing static pressure, $\frac{(PD203) (P_T)}{144}$, psia
PERCENT WC2	percent corrected airflow, $\frac{100(WC2)}{217}$
PH	phase
PREF	Kulite and scanivalve reference pressure, psf
PT	free-stream total pressure, psf
PT1	nose boom total pressure ratio, $\frac{\text{boom pressure}}{P_T}$
PT2	average compressor face total pressure, psf
(PT2R/PT2)BASE	base radial profile for ring 1 through ring 5, respectively
(PT2R/PT2)MEAS	measured radial profile for ring 1 through ring 5, respectively
P3	average throat plug exit pressure, psf
P30e	throat plug exit pressure ratios, e = tap number, $\frac{\text{exit pressure}}{P_T}$
PTRMS	average compressor RMS total pressure ratio, $\frac{\text{average compressor RMS pressure}}{P_T}$
Q	free-stream dynamic pressure, psf
QI/PT2	ratio of average inlet dynamic pressure to average compressor face total pressure

<u>Symbol</u>	<u>Definition</u>
Rf _{gg}	duct boundary-rake total pressure ratios, f = rake number, gg = probe number, $\frac{\text{rake pressure}}{PT}$
RN/FT	Reynolds number, millions/ft
RUN	run number
SEQ	data sequence number
SPF _h	forebody static pressure ratios, h = tap number, $\frac{\text{forebody pressure}}{PT}$
THETA	circumferential extent of distortion for ring 1 thru 5, respectively
TN	tunnel, 14 = Ames 14-Foot Transonic Wind Tunnel
TR	free-stream static temperature, °R
TST	test number
TTR	free-stream total temperature, °R
VIA _{xL}	actual blowing velocity, ft/sec, x - 1 = lip, 2 = diffuser
VIA _{x0}	theoretical blowing velocity, x - 1 = lip, 2 = diffuser
WAX	blowing air weight flow, lb/sec, x - 1 = lip, 2 = diffuser
WC2	duct full scale corrected weight flow, lb/sec
W2	model duct flow, lb/sec

MODEL DESCRIPTION

Shown in figure 1 is the 15-percent-scale pressure model installed in the Ames 14-Foot Transonic Wind Tunnel. The model (fig. 2) consisted of a removable forebody assembly, an underslung inlet and subsonic duct with a simulated compressor face, and a remotely controlled conical-plug flow meter. The forebody (fig. 3) was removed for isolated inlet testing. The inlet (fig. 4) was a two-dimensional, horizontal-ramp system with a 6-degree initial ramp angle. A section of the inlet cowl was removable, allowing incorporation of the three different leading-edge devices. The entire forebody and inlet assembly was mounted on a remotely actuated pitch/yaw mechanism (fig. 5) which, in turn, was mounted on the wind tunnel model-support-system. This combination provided a capability of 56° angle of attack and 15° angle of sideslip.

The inlet cowl leading-edge devices consisted of a flap (fig. 6) deflected 0° , 30° or 50° , a slotted flap (fig. 7) deflected 30° , 45° or 60° , and a tangential blowing slot (fig. 8). Diffuser wall blowing jets, which were used independently and in combination with the leading-edge devices, are described in figure 4. It should be noted that the drawings are to scale, with only limited dimensions being given.

INSTRUMENTATION

Steady state pressure instrumentation in the inlet subsonic-diffuser duct consisted of five total pressure boundary-layer rakes mounted downstream of the cowl-lip (fig. 9) and wall-static orifices on or near the duct centerline on both the ramp and cowl surfaces as well as near each rake location (fig. 10). Instrumentation at the simulated compressor face (fig. 11) consisted of 40 steady state and 40 high-response total pressure probes located on centroids of equal area. Kulite XDBL-093-25 pressure transducers were used to make high response measurements at the compressor face. A Kulite XCQ-093-25 pressure transducer mounted in the nose of the removable forebody was used to monitor the wind tunnel turbulence. Dynamic data were recorded on the NASA Ames high-response data acquisition system (ref. 1). All steady state pressures were measured with a multi-pressure scanning valve assembly mounted on the model support.

TESTING AND PROCEDURE

The variation of engine-face total pressure recovery and distortion with inlet mass-flow ratio was established for each model configuration and test condition. All runs were made at constant Mach number and model attitude while the inlet mass flow was varied using the remotely-controlled,

conical-plug flowmeter. The number of data points for each model configuration and test condition varied from one to seven with at least one engine match point (based on the Pratt and Whitney Aircraft F100-PW-100(3) turbofan engine).

For each data point, tunnel and model conditions were set and 45 seconds of dynamic data were recorded on the NASA Ames high-response data acquisition system. Steady state data were then recorded.

Estimated uncertainties of the primary parameters, based on the accuracy of the measuring instrumentation and repeatability of data check points, are as follow:

$$\begin{array}{ll} \alpha = \pm 0.1 \text{ DEG.} & \text{PT2/PT} = \pm 0.005 \\ \beta = \pm 0.1 \text{ DEG.} & \text{AO/AI} = \pm 0.02 \\ \text{M} = \pm 0.005 & \end{array}$$

RESULTS AND DISCUSSION

The run schedule for the present investigation is shown in table 1 and a sample of the tabulated data is shown in the appendix. A complete listing of the tabulated data is not presented in this report because of the large volume required. The data are available from NASA Ames Research Center, Moffett Field, California. Selected plots of the data are presented in figures 12 through 16.

For the isolated inlet, engine-face pressure recovery and steady state distortion as functions of inlet capture-area ratio and the angle of attack are presented for the basic cowl lip and each of the four inlet devices at a Mach number of 0.9 only. All data are for $\beta = 0^\circ$. Performance of the inlet with the basic cowl lip is shown in figure 12 from $\alpha = 0^\circ$ to 56° . Performance is maintained up to $\alpha = 20^\circ$ with a slight decrease in total pressure recovery at $\alpha = 30^\circ$ and progressively increasing losses at $\alpha = 40^\circ$ and 56° . Engine-face distortion increases with decreasing pressure recovery.

A comparison of inlet performance between the basic cowl lip and various cowl-lip flap deflections for inlet angles of attack of 30° , 40° , and 56° is shown in figure 13. At $\alpha = 30^\circ$ (fig. 13a), the 30° flap deflection provides a small increase in total pressure recovery and little change in distortion. The 50° flap deflection provides no increase in pressure recovery, and distortion at the lower capture-area ratios is increased. At $\alpha = 40^\circ$ (fig. 13b) with a 30° flap deflection, large increases in total pressure recovery are seen along with a decrease in distortion. The 50° flap deflection at $\alpha = 40^\circ$ also improves the inlet performance; however, the increase is only about one-half of that achieved with the 30° flap deflection. The distortion with the 50° flap deflection is improved

at the high capture-area ratios but increased at the lower values. At $\alpha = 56^\circ$ (fig. 13c) no data are available with the 30° flap deflection, but a marked improvement in performance can be seen with the 50° flap deflection. Approximately a 7% increase in total pressure recovery is achieved at the engine match point. An improvement in engine-face distortion is also realized.

A comparison of the inlet performance for the basic cowl lip and slotted cowl flap is shown in figure 14 at $\alpha = 30^\circ$, 40° , and 56° . At $\alpha = 30^\circ$ (fig. 14a) there is a very small increase in total pressure recovery with the slotted flap deflected 30° and no improvement in engine face distortion. A slotted flap deflection of 45° provided no increase in pressure recovery but did result in a slight improvement in distortion. At $\alpha = 40^\circ$ (fig. 14b) each position of the slotted flap (30° , 45° and 60° deflection) improved the inlet total pressure recovery. The 30° deflection resulted in the greatest gain in performance and the 60° deflection the least. Generally, the engine face distortion was reduced with all slotted flap deflections; however, an increase in distortion can be seen at the lower capture-area ratios for the 60° slotted flap deflection. At $\alpha = 56^\circ$ (fig. 14c) all slotted flap positions improved the inlet performance significantly with the 60° deflection showing the greatest improvement and the 30° deflection the least. In addition to significant increases in total pressure recovery, the use of the slotted flap also resulted in a 0.05 increase in mass flow ratio. The engine face distortion was reduced in all cases.

The inlet performance achieved with tangential blowing at the cowl lip or discrete jet-nozzle blowing in the diffuser is compared to the basic cowl lip data in figure 15 over the angle of attack range. Data are shown at the engine match point with maximum blowing only for each of the devices. The tangential blowing at the cowl lip improves the total pressure recovery from 1.0 to 2.5 percent and decreases the engine-face distortion through most of the angle of attack range. The diffuser blowing provides slightly better total pressure recovery than tangential lip blowing at the high angles of attack; however, the engine face distortion is also increased at the higher angles.

The effect of an aircraft forebody on the performance of the basic inlet is shown in figure 16 from $\alpha = 0^\circ$ to $\alpha = 40^\circ$. No data for $\alpha = 56^\circ$ were available. At angles of attack of 0° (fig. 16a), 20° (fig. 16b), and 30° (fig. 16c), essentially no change in total pressure recovery or distortion was measured. At $\alpha = 40^\circ$ (fig. 16d), however, significant improvements in total pressure recovery (up to 3.5 percent) and reduction in distortion were achieved.

CONCLUDING REMARKS

The performance characteristics of four inlet devices (cowl-lip leading-edge flaps, slotted flaps, tangential blowing and discrete jet-nozzles in the subsonic diffuser) designed to prevent or delay cowl-lip boundary-layer separation or to improve the inlet internal-flow characteristics at high angles of attack were investigated at Mach numbers of 0.7, 0.9 and 1.04.

All of the inlet devices tested are capable of improving inlet performance at high angles of attack. However, parametric studies of each concept are required if optimum effectiveness is to be achieved.

Ames Research Center
National Aeronautics and Space Administration
Moffett Field, Calif. 94035

March 10, 1977

REFERENCES

1. Garner, J. E.: Advanced Inlet/Airframe Integration Test of a 0.15-Scale Inlet Model in the NASA Ames 14-Foot Transonic Tunnel, Volume II: Report No. FZT-636-001, General Dynamics, Fort Worth Division, Fort Worth, Texas, December 1975.

TABLE 1. - RUN SCHEDULE

<u>ALPHA</u>	<u>SCHEDULES</u>	<u>NOTATION</u>
A1	15, 20	
A2	20, 30, 40, 50, 56	
A3	20, 30, 40, 50, 52, 56	
A4	0, 5, 10, 15, 20, 25, 30, 35, 40, 45, 50, 56	

BETA SCHEDULES

B1	0, 5, 10, 15
B2	5, 10, 15
B3	0, 10
B4	5, 10
B5	10, 15
B6	0, 15
B7	0, 5

WC2 SCHEDULES

W1	227, 218, 203, 187, 169, 151, 140
W2	227, 211, 187, 162, 140
W3	227, 211, 140
W4	227, 140
W5	244, 235, 227, 212, 140
W6	244, 227, 140
W7	235, 227

PA1 SCHEDULES

L1	23, 32, 50, 67, 84, 102
L2	32, 67, 102
L3	air off, 32, 50, 67, 84, 102, 119, 136
L4	32, 50, 67, 84, 119, 136
L5	32, 67, 102, 136
L6	air off, 32, 50, 67, 84, 119, 136
L7	air off, 32, 50, 67, 102, 136
L8	air off, 32, 67, 102, 136

PA2 SCHEDULES

C1	37, 48, 60, 105, 150, 195, 240
C2	air off, 60, 150, 195, 240
C3	37, 60, 105, 150, 195, 240
C5	60, 105, 150, 195, 240
C6	air off, 60, 105, 150, 195, 240
C7	air off, 60, 150, 240
C10	60, 150, 240

TABLE 1. - Continued.

- B Forebody
- F_x Cowl flap, x = flap angle, deg
- I Plain cowl lip
- L Blowing lip
- S_x Cowl slotted flap (slat), x = flap angle, deg
- W Boundary layer rakes and diffuser blowing hardware installed in duct

Config. Code	Component Notation								
	B	F30	F50	I	L	S30	S45	S60	W
1				X					X
2		X							X
3			X						X
4						X			X
5							X		X
6								X	X
7					X				X
8	X				X				X
9	X						X		X
10	X		X						X
11	X			X					X
12	X			X					

TABLE 1. - Continued.

RUN	M	ALPHA	BETA	CONF	WC2	PA1	PA2	REMARKS
1	0.7	0	0	1	W1	air off	air off	WC2 out of limits at SEQ 30
2			0		W2			WC2 out of limits at SEQ 38
3			B2		227			
4		10	0		W3			WC2 out of limits at SEQ 45
5		15			W4			WC2 out of limits at SEQ 47
6		20			W4			WC2 out of limits at SEQ 49
7					227		C1	
8			B2				air off	
9		25	0					
10		35	B1					
11		40	0		W4			WC2 out of limits at SEQ 66
12		45	0		227			
13		56	B3					
14		30	0				C2	
15		56					C2	
16		56			140		air off	
17	0.9	0			W1			
18		20						
19		56						

TABLE 1. - Continued.

RUN	M	ALPHA	BETA	CONF	WC2	PA1	PA2	REMARKS
23	0.9	15	0	1	W6	air off	air off	
24		20			W5		air off	
25		20			227		C3	
28	0.9	30	0	1	W6		air off	
29		30	0		227		C2	
30		35	B1		227		air off	
31		40	0		W6			
32		45			227			
33		50			227			
34		56			W6			
35					227		C2	
36			10				air off	
37			15				C2	
38		35	15				C2	
39		45	0				C6	
40		45					air off	
41		20		2	W5		air off	
42					227		C5	
43			B2				air off	
44		25	0				air off	

TABLE 1. - Continued.

RUN	M	ALPHA	BETA	CONF	WC2	PA1	PA2	REMARKS
45	0.9	35	B1	2	227	air off	air off	
46		45	0					
47		50						
48		30			W6			
49		30			227		C5	
50		40			W6		air off	
51		40			227		C5	
52		45			W6		air off	
53		45			227		C5	
54		56			227		C5	
55				3	W6		air off	
56					227		C5	
57		50					air off	
58		45						
59		40			W6			
60		40			227		C5	
61		35	B1		227		air off	
62		30	0		W6		air off	
63		30			227		C5	
64		25			227		air off	
65		20			W5		air off	
66		20			227		C5	

TABLE 1. - Continued.

RUN	M	ALPHA	BETA	CONF	WC2	PA1	PA2	REMARKS
67	0.9	20	B2	3	227	air off	air off	
68		35	15				C5	
69		56	15					
70	0.7	56	0					
71	0.9	20		4	W5		air off	
72					227		C5	
73			B2				air off	
74		25	0					
75		30			W6			
76		30			227		C5	
77		35	B1		227		air off	
78		40	0		W6		air off	
79		40			227		C5	
80		45					air off	
81		50						
82		56			W6			
83					227		C5	
84			15				C6	
85		35	15				C6	
86		56	0	5	W6		air off	
87		56			227		C5	
88		50			227		air off	

TABLE 1. - Continued.

RIN	M	ALPHA	BETA	CONF	WC2	PA1	PA2	REMARKS
89	0.9	45	0	5	227	air off	air off	
90		40			W6		air off	
91		40			227		C6	
92		35	B1		227		air off	
93		30	0		W6		air off	
94		30			227		C6	
95		56		6	W6		air off	
96		56			227		C5	
97		50					air off	
98		45						
99		40			W6			
100		40			227		C5	
101		35					air off	
102	0.7	56					C7	
103		50					air off	
104		45					air off	
105		40					C7	
106	0.9	0		7	W5		air off	
107		0	15		227			
108		10	0					
109		15						
110		20			W5			

TABLE 1. - Continued.

RUN	M	ALPHA	BETA	CONF	WC2	PA1	PA2	REMARKS
111	0.9	20	0	7	227	L1	air off	
112			B2			air off		
113			15			L2		
114		25	0			L3		Regulator leakage PA2 = 22, SEQ 657-663
115		30			W6	air off		
116		30			227	L4		Regulator leakage PA2=18, SEQ 668&669
117		35				L3		
118			B2			air off		
119			15			L5		
120			15			67	C7	
121		30	0			50	C6	
122		40			W6	air off	air off	
123		40			227	L4		Regulator leakage, PA2=15, SEQ 717-721
124		45				L6		
125		50				L6		
126		56				L7		
127						67	C6	
128						136	C6	
129					SELECT	67	air off	WC2=215,200,182
130					182	136		
131		45			227	SELECT		PA1=air off,67,136
132		45			215	67		

TABLE 1. - Continued.

RUN	M	ALPHA	BETA	CONF	WC2	PA1	PA2	REMARKS
133	0.9	40	0	7	159	L8	air off.	
134					203			
135					214			
136					228			
137					SELECT	102	240	WC2=228, 214, 203
138		50			227	L8	air off	
139					212			
140					203			
141	0.7	40			219			
142					213			
143					204			
144					SELECT	102	240	WC2=204, 213
145	0.9	56		8	227	L8	air off	
146		56			204			
147		50			227			
148		50			203			
149		40			203			
150					212			
151					227			
152	1.04							
153	1.04	35						
154	0.9	40			SELECT	67	240	WC2=228, 213, 203

TABLE 1. - Continued.

RUN	M	ALPHA	BETA	CONF	WC2	PA1	PA2	REMARKS
155	0.9	35	0	8	227	L8	air off	
156		30		8	227	air off		
157		56		9	W6			
158		56			227		C10	
159		50					C7	
160		45					air off	
161		40			W6		air off	
162		40			227		C10	
163		35					air off	
164		30					C7	
165		25					air off	
166		20			W6		air off	
167					227		C10	
168			B2				air off	
169			15				240	
170		35	B2				air off	
171		35	15				C10	
172	1.01	56	0				C7	
173	0.7	56						
174		50						
175		40						
176	0.9	56		10	W6		air off	

TABLE 1. - Continued.

RUN	M	ALPHA	BETA	CONF	WC2	PA1	PA2	REMARKS
177	0.9	56	0	10	227	air off	C10	
178		50					C7	
179		45					air off	
180		40			W6		air off	
181		40			227		C10	
182		35					air off	
183		30					C7	
184		25					air off	
185		20			W6		air off	
186		20			227		C10	
187	0.7	50		3			C7	
188		45					air off	
189		40			W6		air off	
190		40			W6		C10	
191		35			227		air off	
192		30					C7	
193		25					air off	
194		20			W6		air off	
195		20			227		C10	
196		35	15				C7	
197		35	B4				air off	
198		56	B4				air off	

TABLE 1. - Continued.

RUN	M	ALPHA	BETA	CONF	WC2	PA1	PA2	REMARKS
199	0.7	56	15	3	227	air off	C10	
200		45	15				C7	
201		45	B2				air off	
202		56	0				240	
203		56		2			C7	
204		50					C7	
205		45					air off	
206		40					C7	
207		35					air off	
208		30					C7	
209		25					air off	
210		20					C7	
211		45	15				C7	
212		45	B2				air off	
213		56	B1				air off	
214		56	15				C10	
215		35	15				C7	
216		35	B5				air off	
217	0.9	56	0				air off	
218	0.9		15				SELECT	PA2=air off,10
219	0.7		0	5			C7	
220	0.7	50	0	5			C7	

TABLE 1. - Continued.

RUN	M	ALPHA	BETA	CONF	WC2	PA1	PA2	REMARKS
221	0.7	45	0	5	227	air off	air off	
222		40					C7	
223		35					air off	
224		30					C7	
225		25					air off	
226		20					C7	
227			15				C7	
228			B4				air off	
229		56	B4				air off	
232	0.7	45	B4	5	227	air off	air off	
233		50	0	4			C7	
234		45					air off	
235		40					C7	
236		35					air off	
237		30					C7	
238		56					C7	
239		25					air off	
240		20					C7	
241		45	15				C7	
242		45	B4				air off	

TABLE 1. - Continued.

RUN	M	ALPHA	BETA	CONF	WC2	PA1	PA2	REMARKS
243	0.9	0	0	1	W5	air off	air off	
244			5		W7			
245			10					
246			15					
247		5	0					
248		10	0					
249			5					
250			10					
251			15					
252		A1	0		235			For 2nd point of run BETA = 5
253		20	5		W7			
254		20	10		W7			
255		0	0	11	W5			
256		0	B2		227			
257		10	0		W6			
258		15			W6			
259		20			W5			
260			B2		227			
261			0				C10	
262		25					air off	
263		30			W6		air off	
264		30			227		C10	

TABLE 1. - Continued.

RUN	M	ALPHA	BETA	CONF	WC2	PA1	PA2	REMARKS
265	0.9	35	B1	11	227	air off	air off	
266		40	0		W6		air off	
267		40			227		C10	
268		45					air off	
269		50	B6					
270		56						
271		56					240	
272		50						
273	0.7	A2	0					
274		A3	15					
275		A4	0				air off	
276		56	B4					
277		45	B2					
278		35						
279		20						
280	0.9	0	0	12	W5			
281			B2		227			
282			B2		235			
283		5	0		W7			
284		10	0		W5			
285			B2		227			
286			B1		235			

TABLE 1. - Continued.

RUN	M	ALPHA	BETA	CONF	WC2	PA1	PA2	REMARKS
287	0.9	15	0	12	W7	air off	air off	
288		20	0		W5			
289			B2		227			
290			B2		235			
291		25	0		W7			
292		30	0		W5			
293			B2		227			
294			B2		235			
295		35	0		W7			
296		35	5		W7			
297		40	0		W6			
298		45	B1		227			
299		50	0		W6			
300		56	0		W6			
301		56	B2		227			
302		0	0		W3			
303		0	B2		227			
304		5	0		227			
305		10	0		W3			
306		10	B2		227			
307		15	0		227			
308		20	0		W3			

TABLE 1. - Concluded.

RUN	M	ALPHA	BETA	CONF	WC2	PA1	PA2	REMARKS
309	0.9	5	B2	12	227	air off	air off	
310		25	0		227			
311		30	0		W3			
312		30	B2		227			
313	0.7	0	0					
314		0	B2					
315		5	B7					
316		10	0					
317		10	B2					
318		15	0					
319		20	0					
320		5	B4					
321		20	B2					
322		25	0					
323		30	0					
324		30	B2					
325		35	B7					
326		40	0					
327		40	B2					
328		45	B6					
329		50	0					
330		56	0					
331		56	5					

TABLE 2. - INDEX OF FIGURES

Figure	Title	Page
1	Model installed in Ames 14-foot transonic wind tunnel	28
2	General arrangement of 15 percent scale inlet model	29
3	Model forebody	30
4	Model inlet	31
5	Representative test setups	32
6	Inlet cowl leading-edge flap	33
7	Inlet cowl leading-edge slotted-flap	34
8	Inlet cowl leading-edge tangential blowing slot	35
9	Static-pressure orifice locations in subsonic diffuser	36
10	Boundary-layer rake details	38
11	Compressor-face rake details	39
12	Performance of isolated inlet with basic cowl lip; $M = 0.9$, $\beta = 0^\circ$	40
13	Performance of isolated inlet with cowl flap; $M = 0.9$, $\beta = 0$	41
14	Performance of isolated inlet with slotted cowl flap; $M = 0.9$, $\beta = 0$	44
15	Performance of isolated inlet with tangential blowing cowl slot and diffuser blowing; $M = 0.9$, $\beta = 0$	47
16	Performance of inlet with basic cowl lip and forebody; $M = 0.9$, $\beta = 0$	48

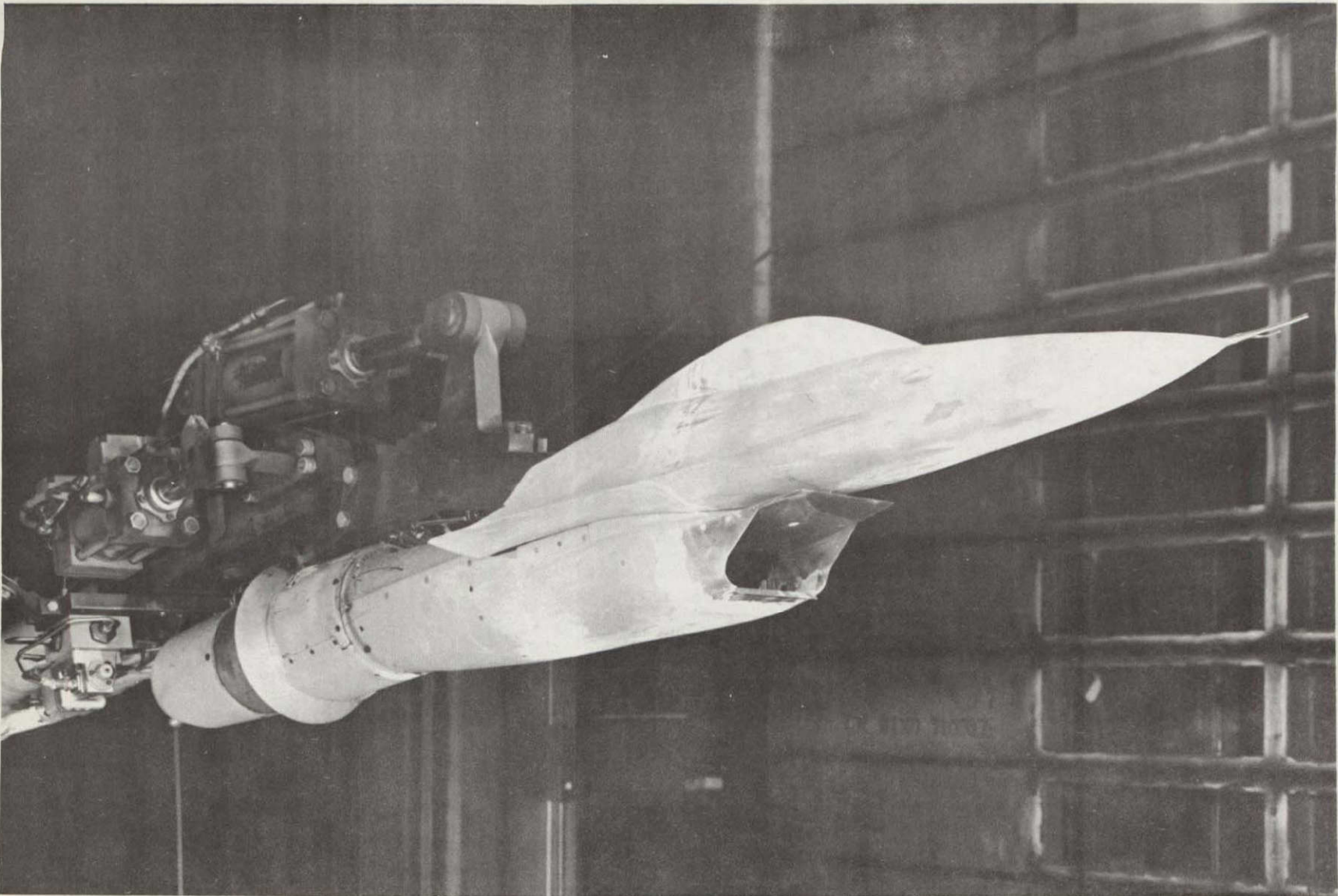


Figure 1. - Model installed in Ames 14-Foot Transonic Wind Tunnel.

ORIGINAL PAGE IS
OF POOR QUALITY

ORIGINAL PAGE IS
OF POOR QUALITY

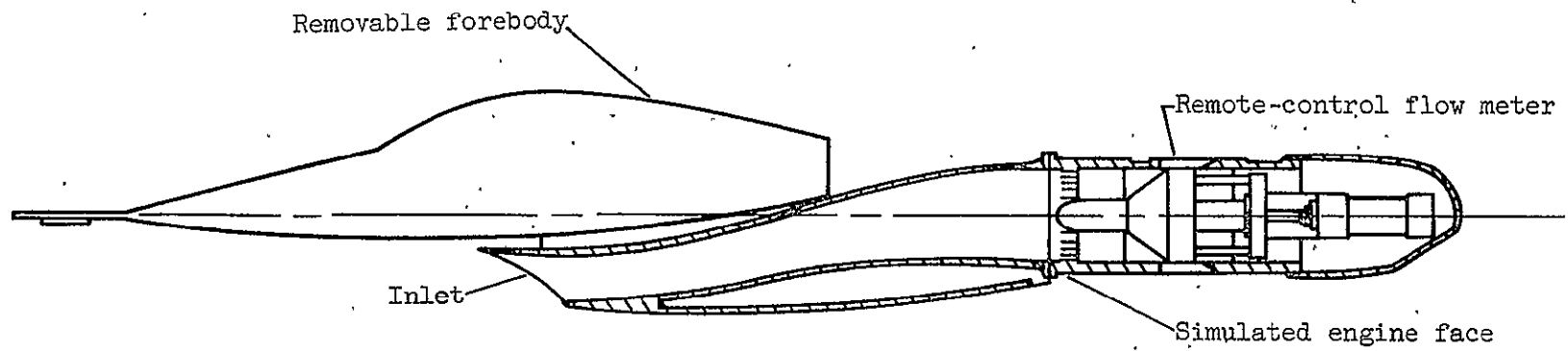


Figure-2. - General arrangement of 15 percent scale inlet model.

Note: All dimensions are
in centimeters

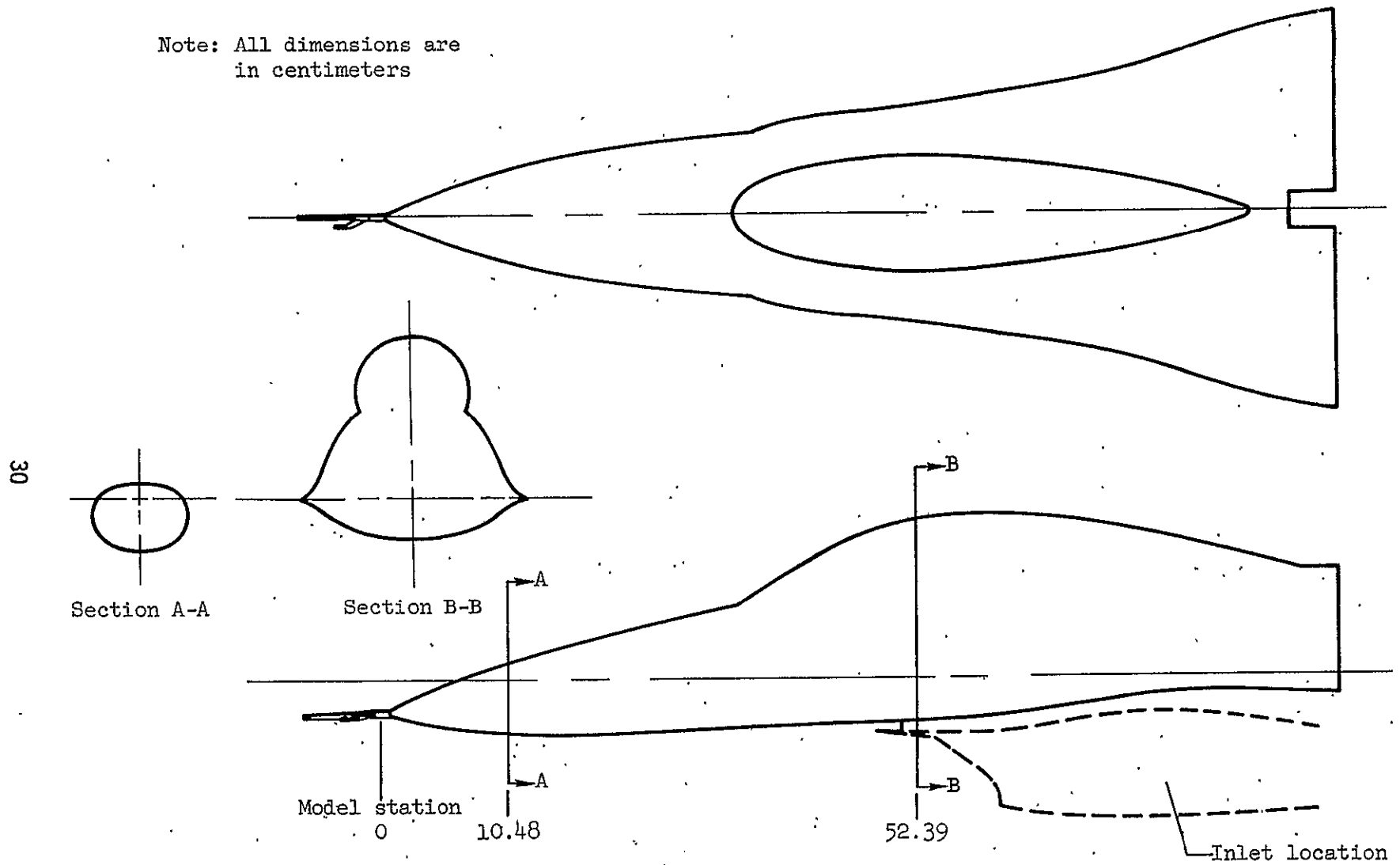
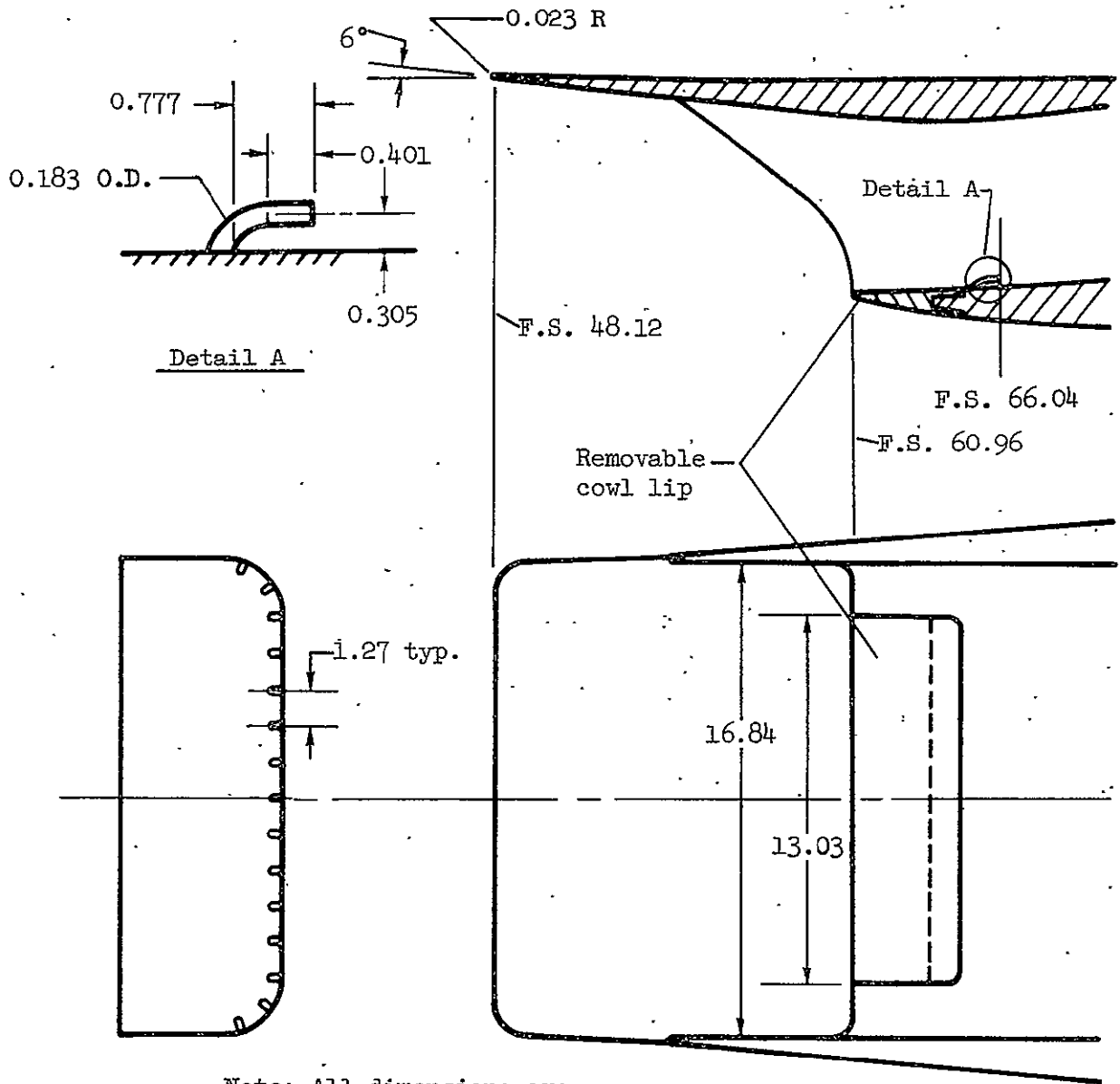


Figure 3. - Model forebody.



Note: All dimensions are in centimeters

Figure 4.- Model inlet.

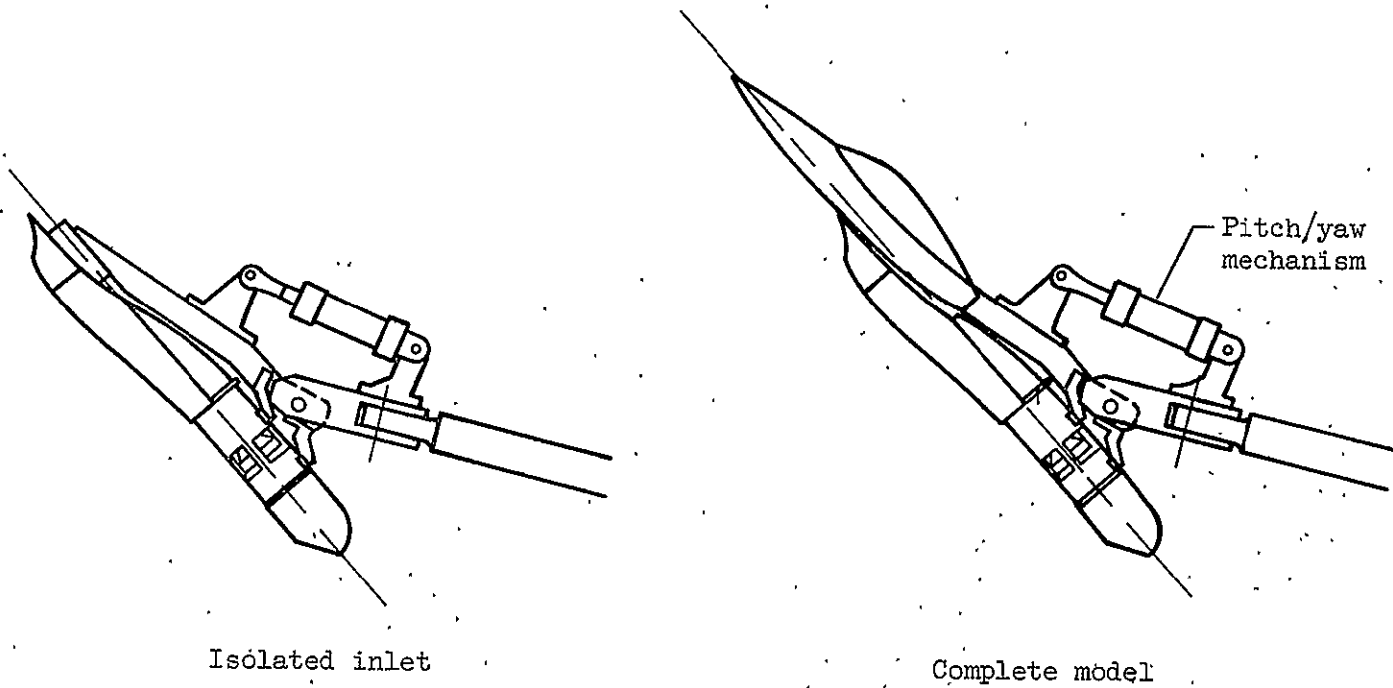
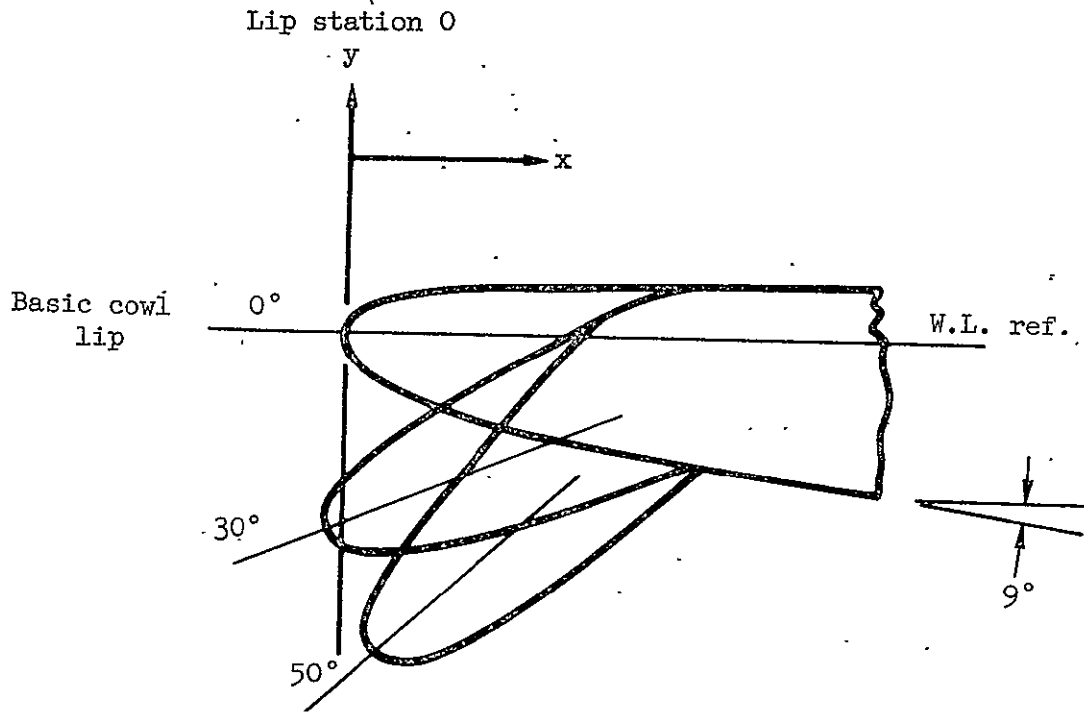


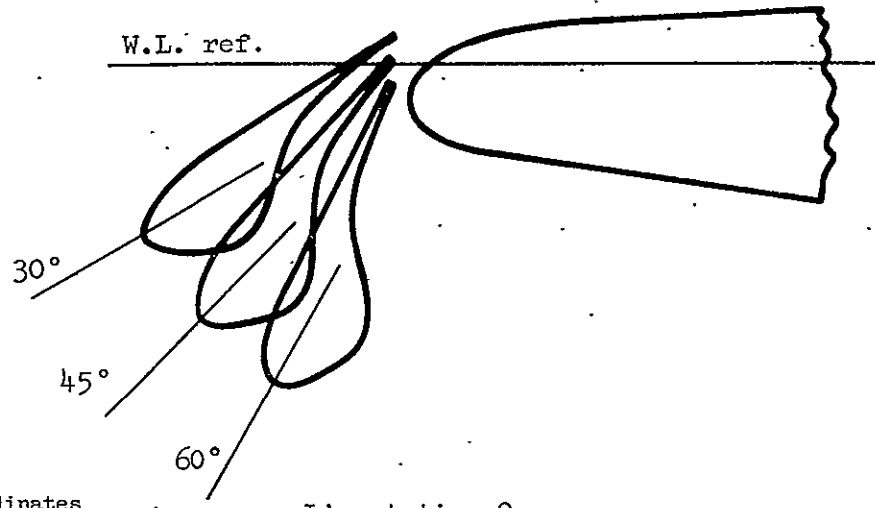
Figure 5.- Representative test setups.



Basic lip and flap ordinates

Basic lip, 0°			30° flap			50° flap		
Lip station, x, cm	Lower surface, y, cm	Upper surface, y, cm	Lip station, x, cm	Lower surface, y, cm	Upper surface, y, cm	Lip station, x, cm	Lower surface, y, cm	Upper surface, y, cm
0	0	0	-0.038	-0.483	-0.483	0.071	-0.800	-0.800
0.043	-0.084	0.053	-0.018	-0.541	-0.437	0.091	-0.846	-0.709
0.102	-0.130	0.079	0.051	-0.569	-0.353	0.127	-0.864	-0.638
0.180	-0.170	0.102	0.102	-0.577	-0.312	0.180	-0.861	-0.554
0.282	-0.206	0.117	0.178	-0.577	-0.254	0.231	-0.853	—
0.381	-0.234	0.124	0.282	-0.556	-0.185	0.282	-0.800	—
0.508	-0.257	0.127	0.348	—	-0.145	0.323	—	-0.368
0.660	-0.282	↑ straight line	0.381	-0.533	↑ straight line	0.381	-0.785	↑ straight line
—	↑ straight line	—	0.508	-0.495	—	0.508	-0.699	—
—	—	—	0.678	-0.434	—	—	—	—
—	—	—	—	↑ straight line	—	0.602	—	—
0.953	-0.328	—	—	—	—	0.632	-0.602	-0.028
1.092	—	0.142	0.721	—	0.071	—	—	—
—	—	—	—	—	—	0.734	-0.516	—
—	—	—	0.953	-0.328	0.140	—	—	—
—	—	—	1.092	—	0.142	—	—	—
—	—	—	—	—	—	—	↑ straight line	—
—	—	—	—	—	—	—	—	—
—	—	—	—	—	—	0.953	-0.328	0.140
—	—	—	—	—	—	1.092	—	0.142

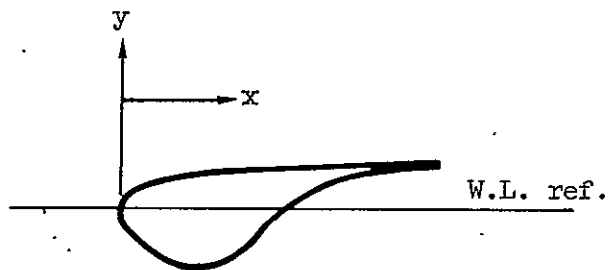
Figure 6.- Inlet cowl leading-edge flap.



Slotted flap ordinates

Lip station, x, cm	Lower surface, y, cm	Upper surface, y, cm
0.023	-0.069	0.043
0.061	-0.099	0.061
0.137	-0.147	0.097
0.259	-0.188	0.119
0.366	-0.155	
0.442	-0.097	↑
0.518	-0.020	straight line
0.594	-0.038	line
0.671	-0.074	↓
0.747	-0.097	
0.899	-0.130	
1.044	-0.142	0.157

Lip station 0



Slotted flap base ordinates

Lip station, x, cm	Lower surface, y, cm	Upper surface, y, cm
0.038	-0.193	-0.033
0.076	-0.231	0
0.152	-0.272	-0.004
0.305	↑	-0.099
0.330	straight line, -9°	-0.130
0.584	↓	-0.140

Lip station 0

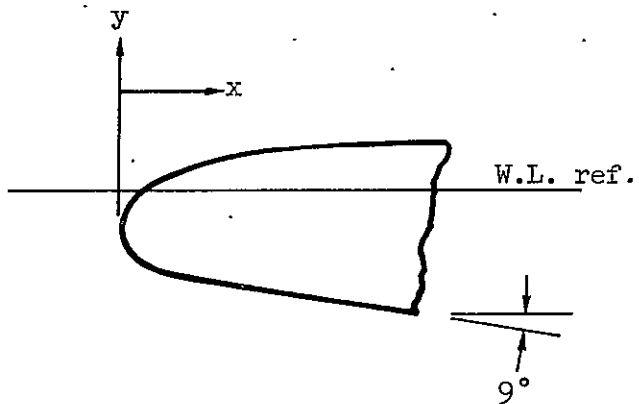
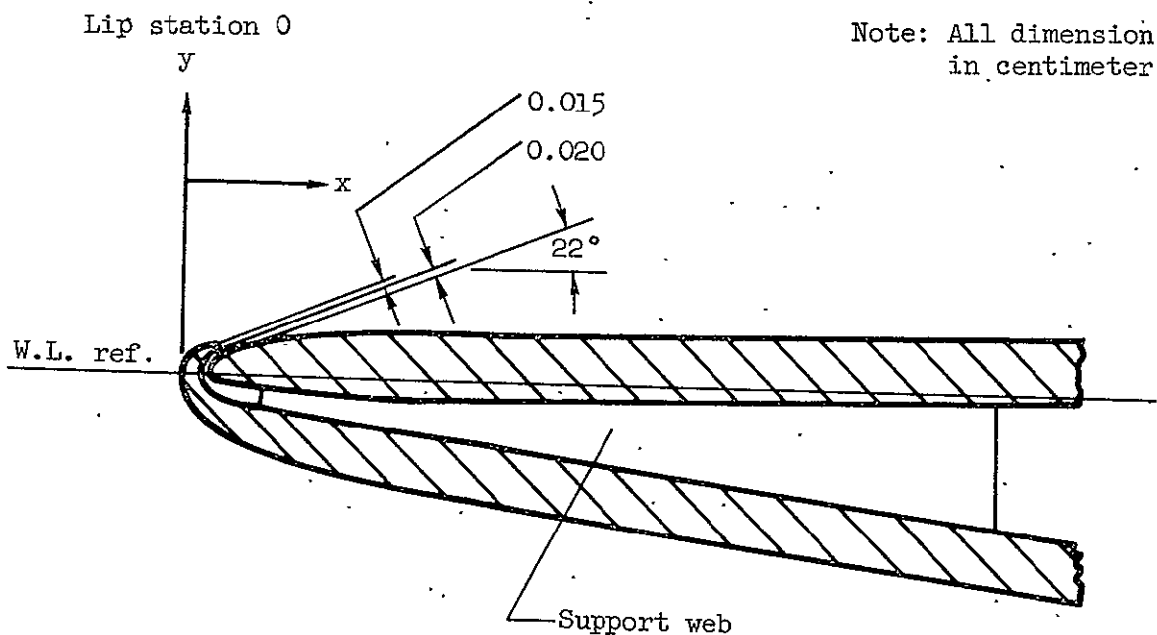


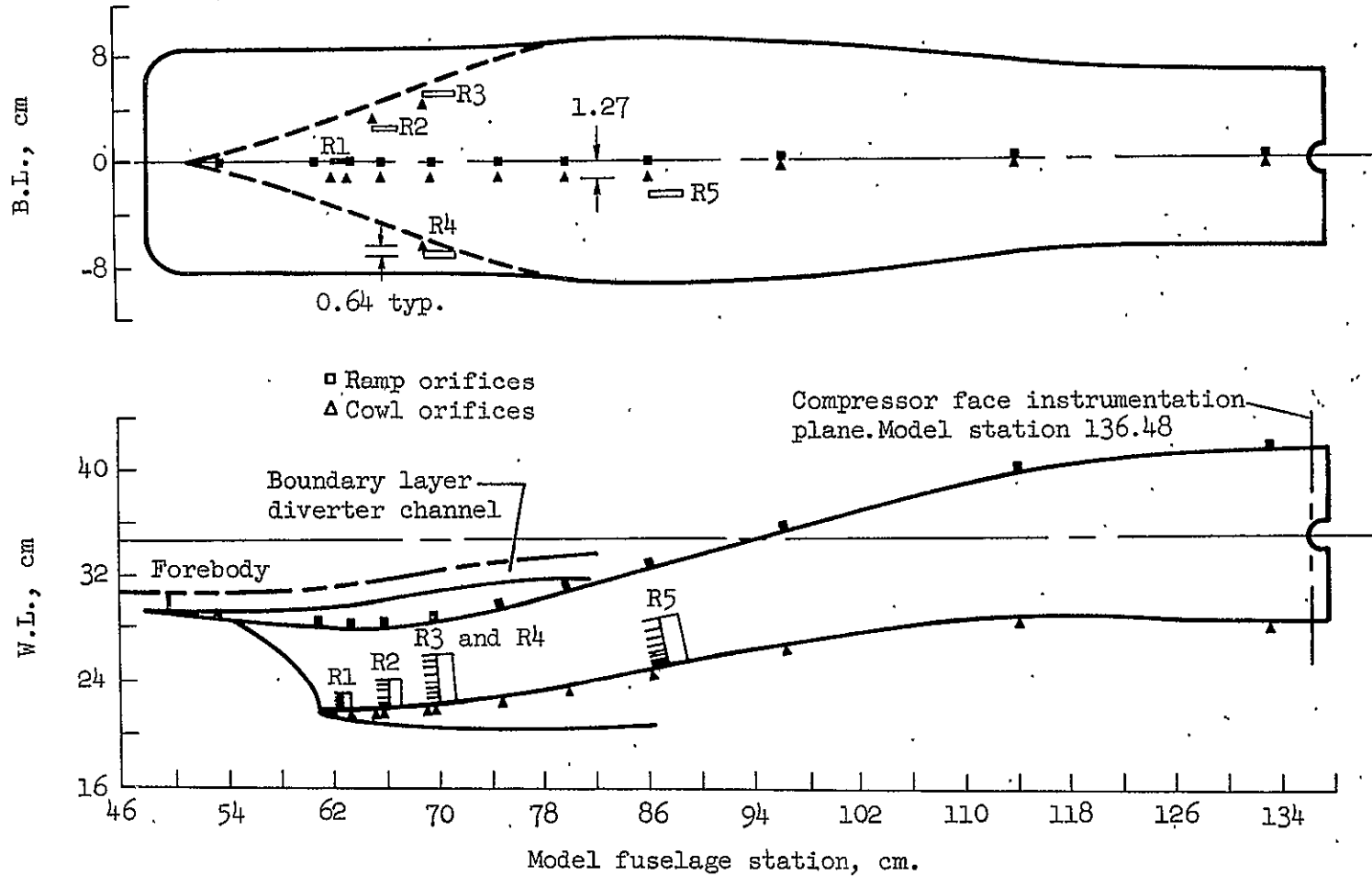
Figure 7.- Inlet cowl leading-edge slotted-flap.



Blowing lip ordinates

Lip station, x, cm	Lower surface, y, cm	Upper surface, y, cm
0.025	-0.079	0.051
0.051	-0.114	0.074
0.102	-0.150	0.086
0.114	—	0.053
0.152	-0.178	—
0.254	-0.208	0.097
0.381	-0.262	0.114
0.508	-0.295	—
0.521	—	0.125
0.635	-0.320	—
0.762	-0.343	—
3.810	straight line, -8°	straight line, 1°

Figure 8.- Inlet cowl leading-edge tangential blowing slot.



(a) Duct instrumentation.

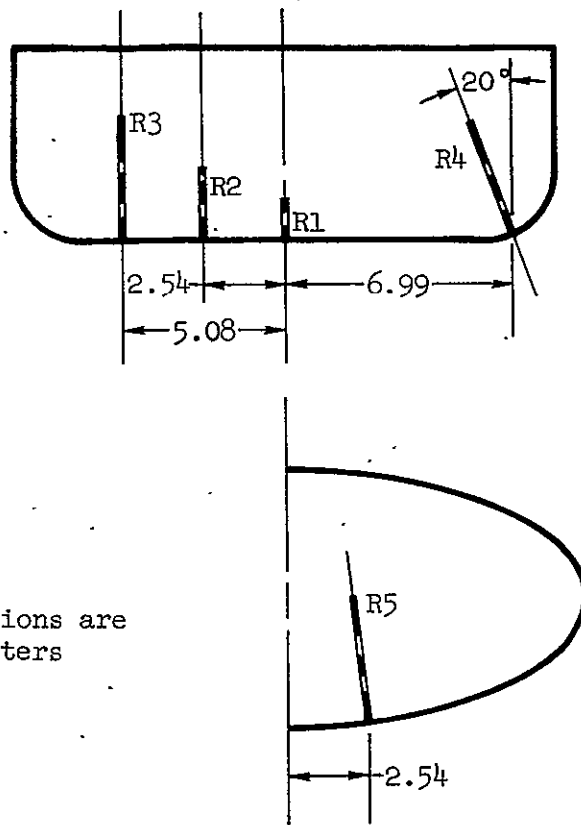
Figure 9.- Static-pressure orifice locations in subsonic diffuser.

Static orifice locations

Ramp orifice no.	Fuselage station, cm	Cowl orifice no.	Fuselage station, cm
D101	53.34	D201	62.23
D102	60.96	D202	63.37
D103	63.50	D203	65.41
D104	66.04	D204	66.04
D105	69.85	D205	69.22
D106	74.93	D206	69.22
D107	80.01	D207	69.85
D108	86.36	D208	74.93
D109	96.52	D209	80.01
D110	114.30	D210	86.36
D111	133.35	D211	96.52
—	—	D212	114.30
—	—	D213	133.35

(b) Static orifice locations.

Figure 9.- Concluded.

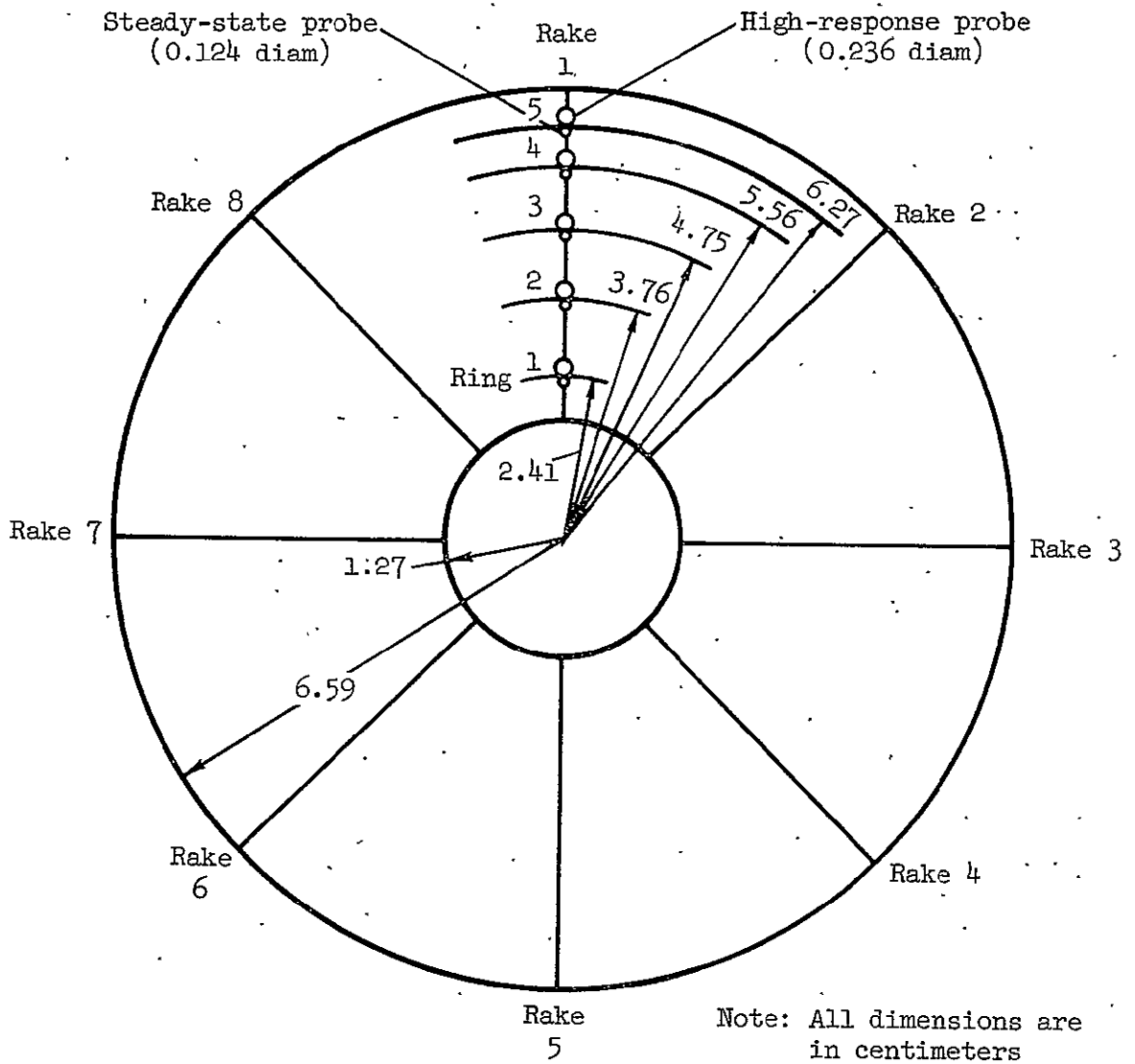


Note: All dimensions are in centimeters

Rake tube locations

Rake R1 Station 62.23	Rake R2 Station 65.41	Rake R3 Station 69.22	Rake R4 Station 69.22	Rake R5 Station 86.36	Height, cm
R101	R201	R301	R401	R501	0.046
R102	R202	R302	R402	R502	0.173
R103	R203	R303	R403	R503	0.351
R104	R204	R304	R404	R504	0.579
R105	R205	R305	R405	R505	0.884
R106	R206	R306	R406	R506	1.265
—	R207	R307	R407	R507	1.722
—	R208	R308	R408	R508	2.256
—	—	R309	R409	R509	2.967
—	—	R310	R410	R510	3.805

Figure 10.- Boundary-layer rake details.



Instrumentation plane; Model station 136.48

Figure 11. - Compressor face rake details

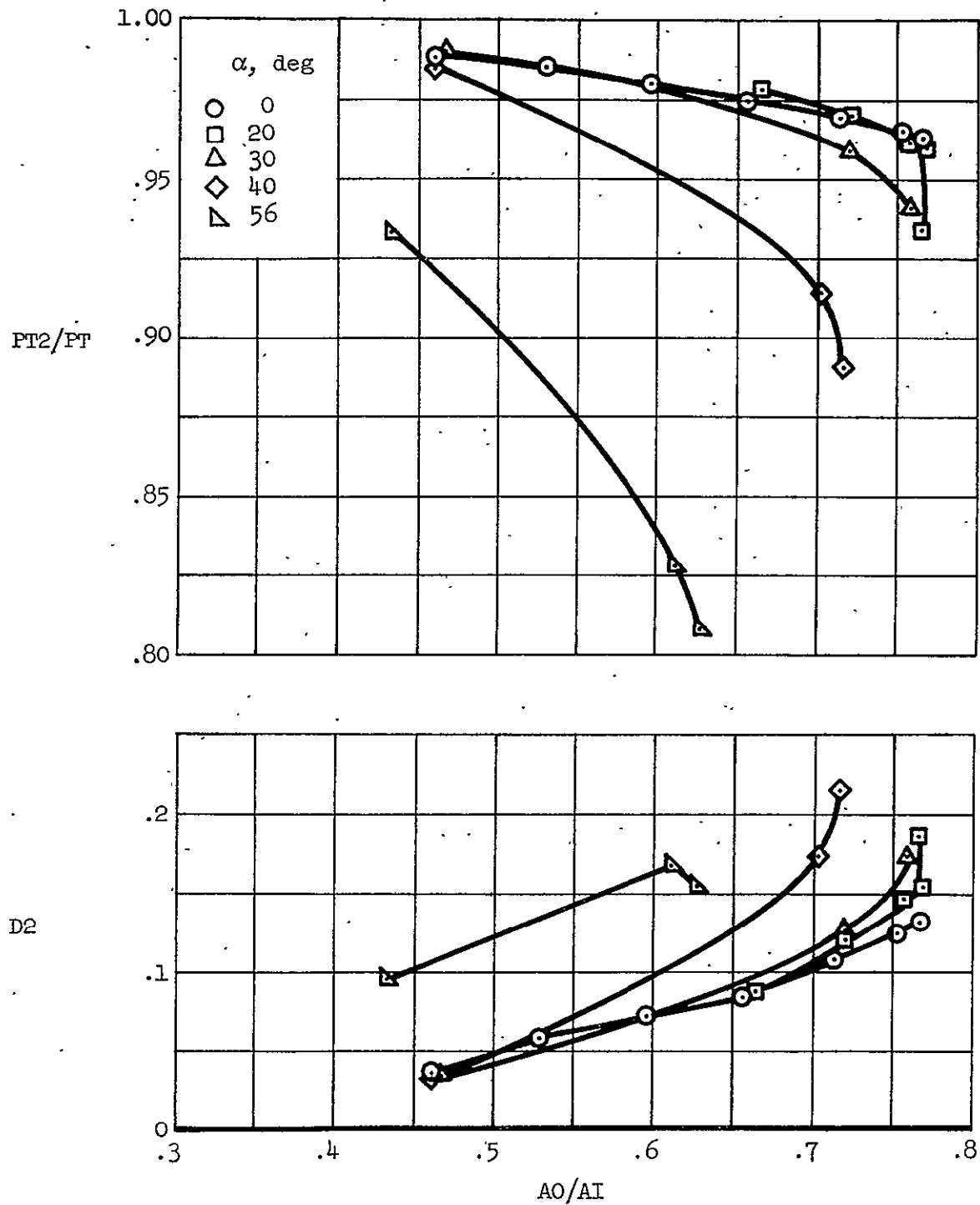
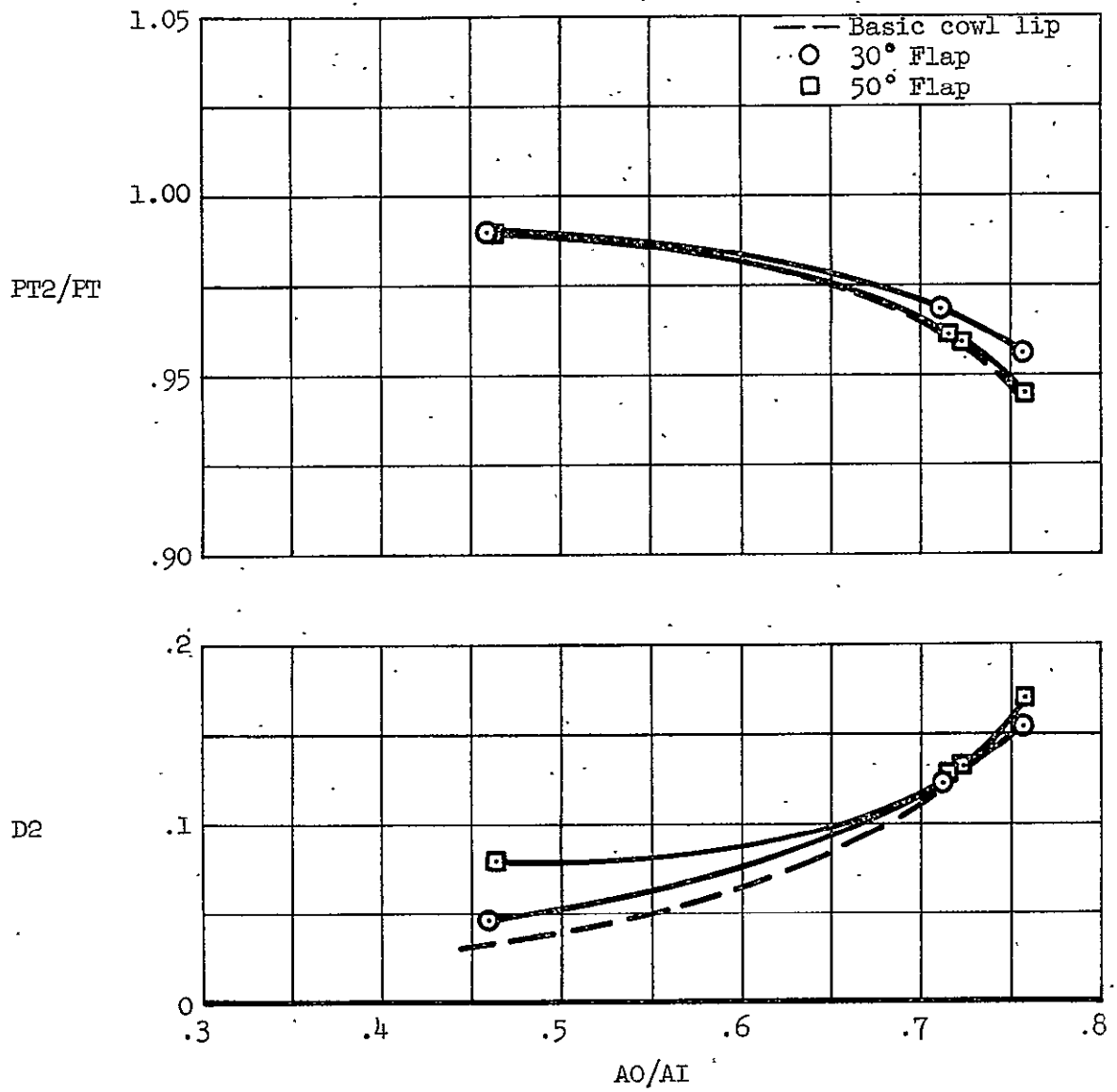
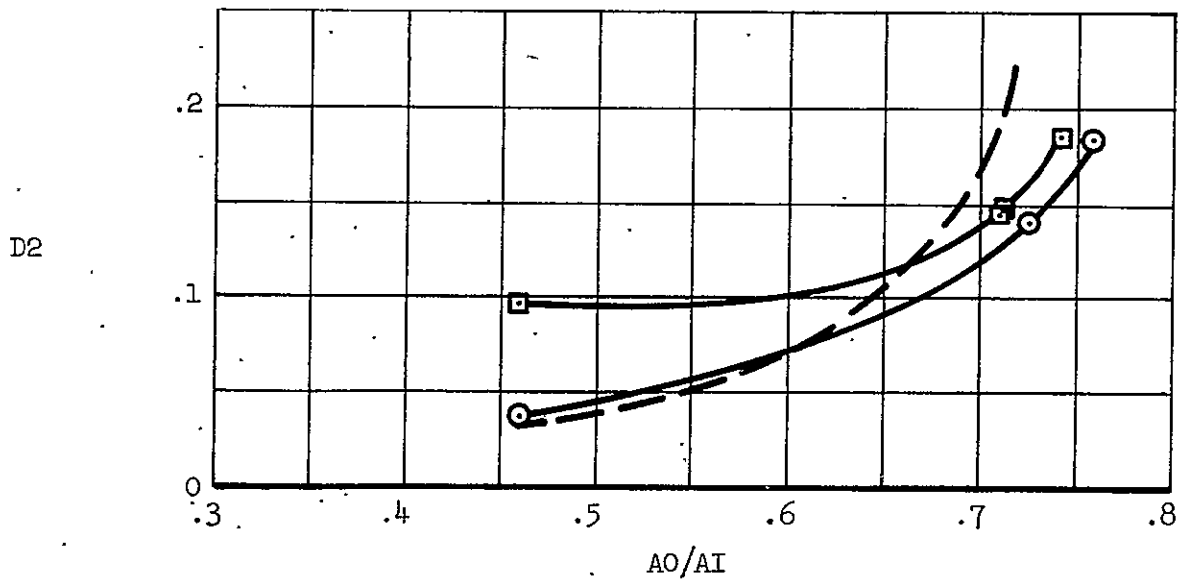
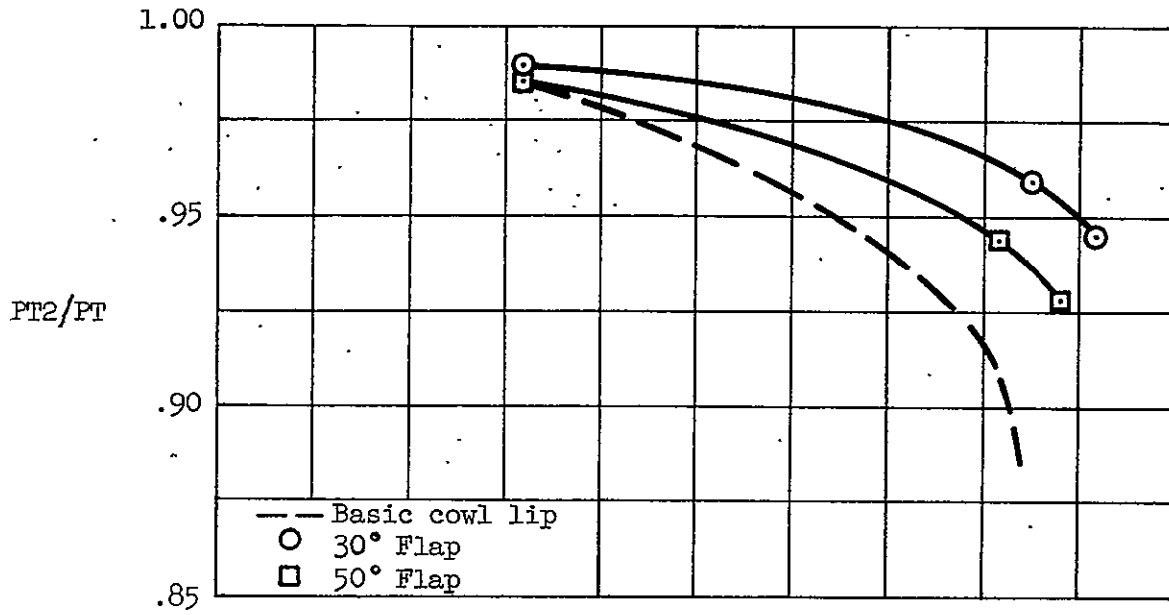


Figure 12.- Performance of isolated inlet with basic cowl lip; $M = 0.9$, $\beta = 0^\circ$.



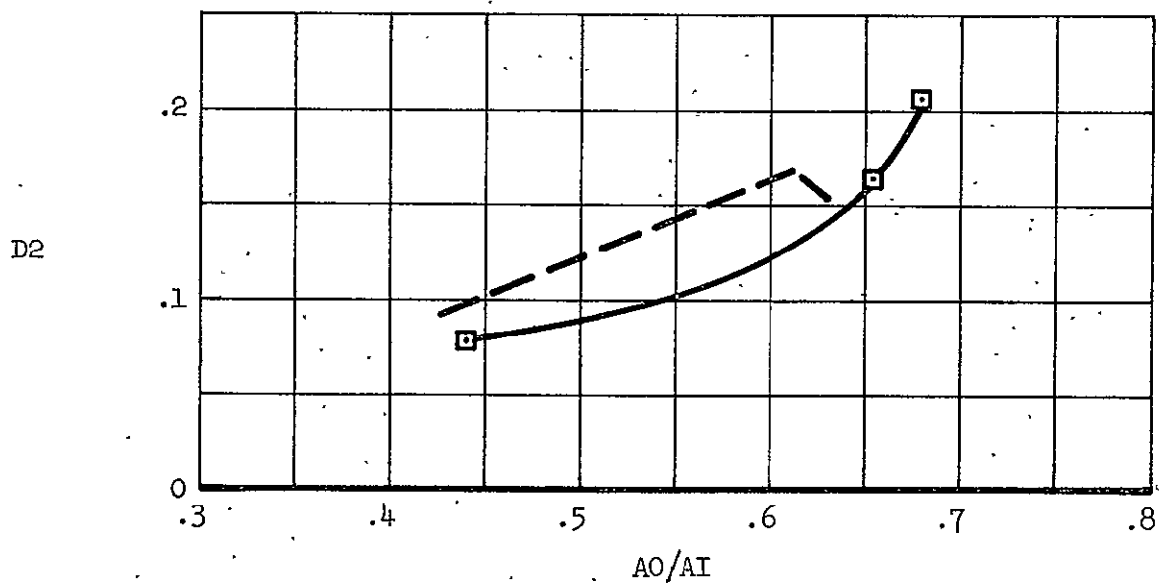
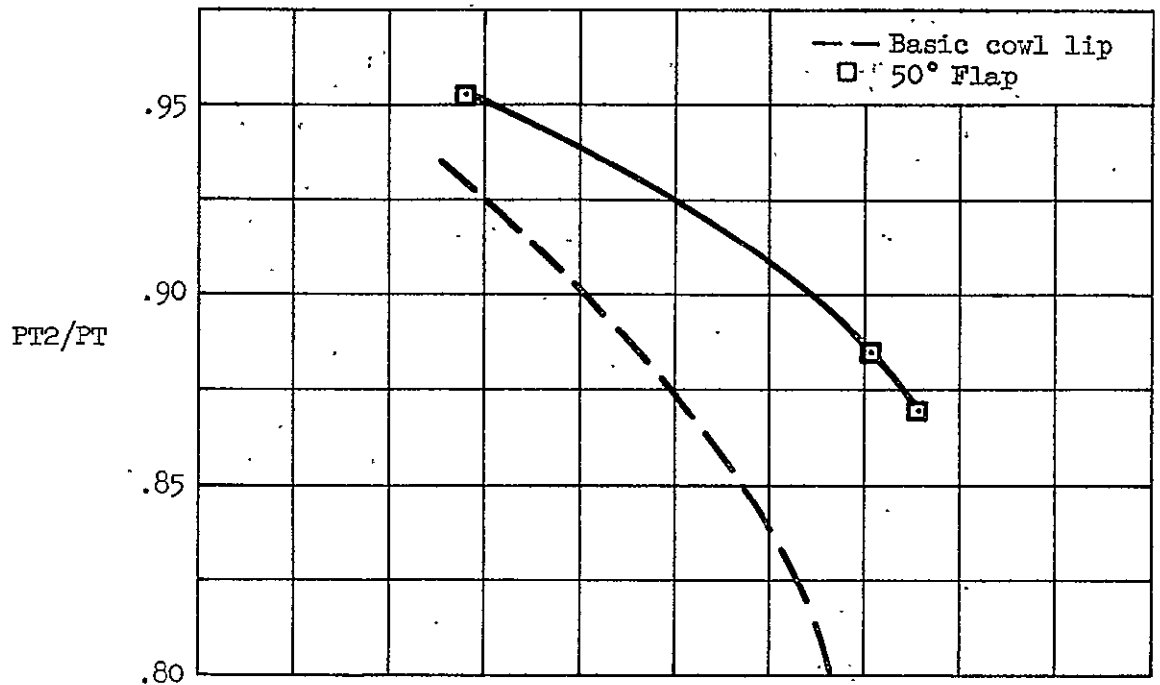
(a) $\alpha = 30^\circ$

Figure 13.- Performance of isolated inlet with cowl flap; $M = 0.9$,
 $\beta = 0^\circ$.



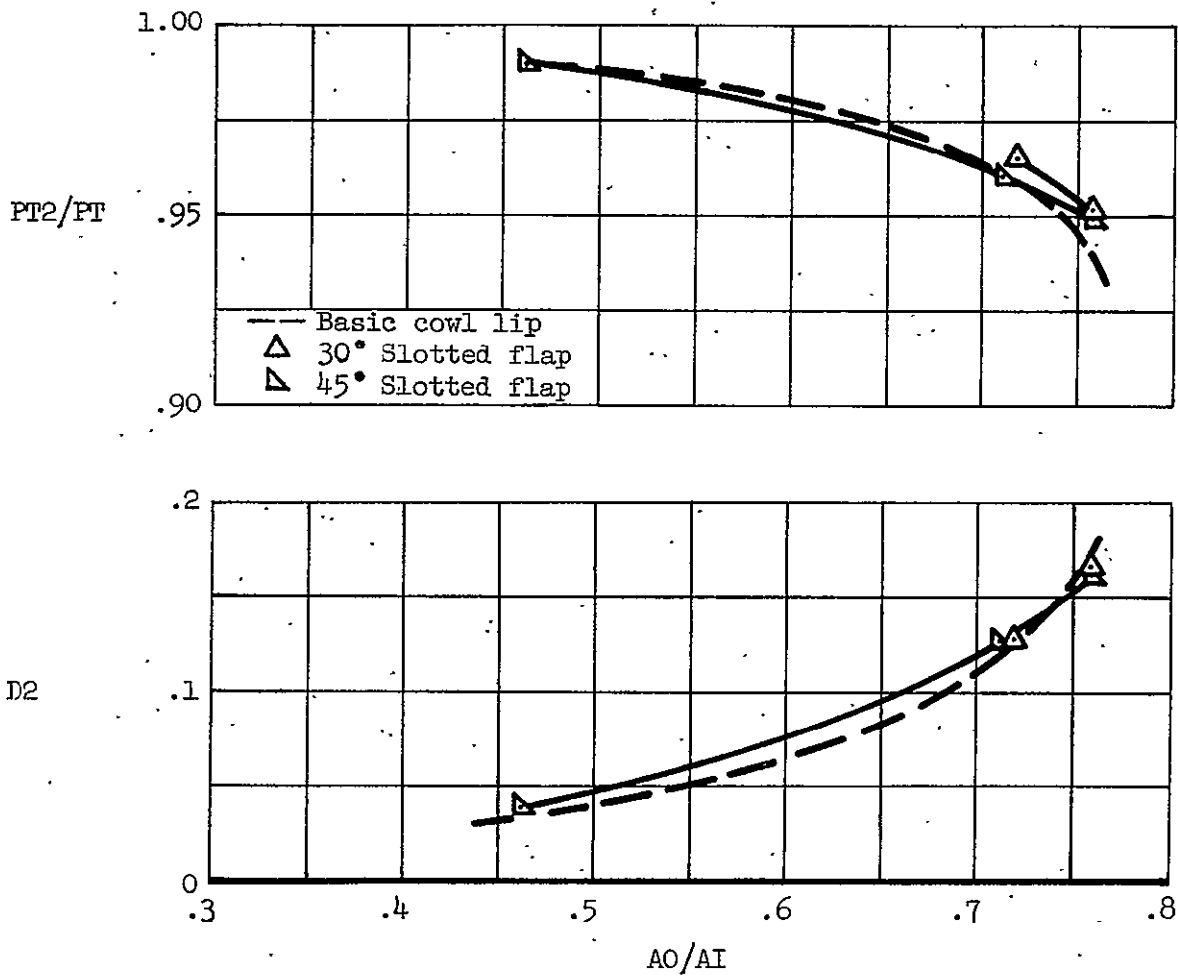
(b) $\alpha = 40^\circ$

Figure 13.- Continued.



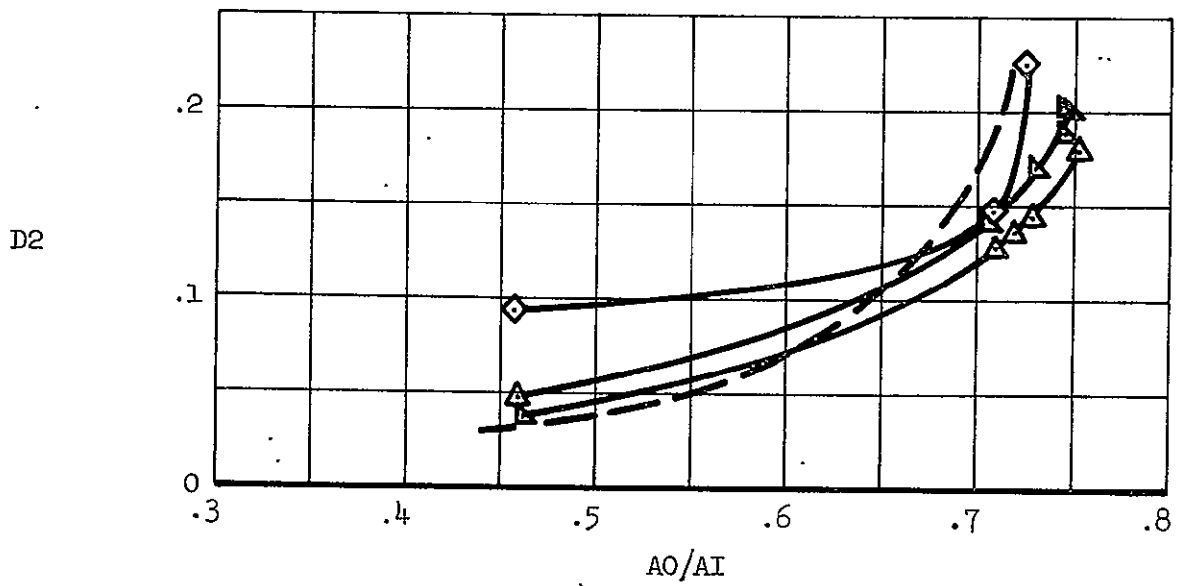
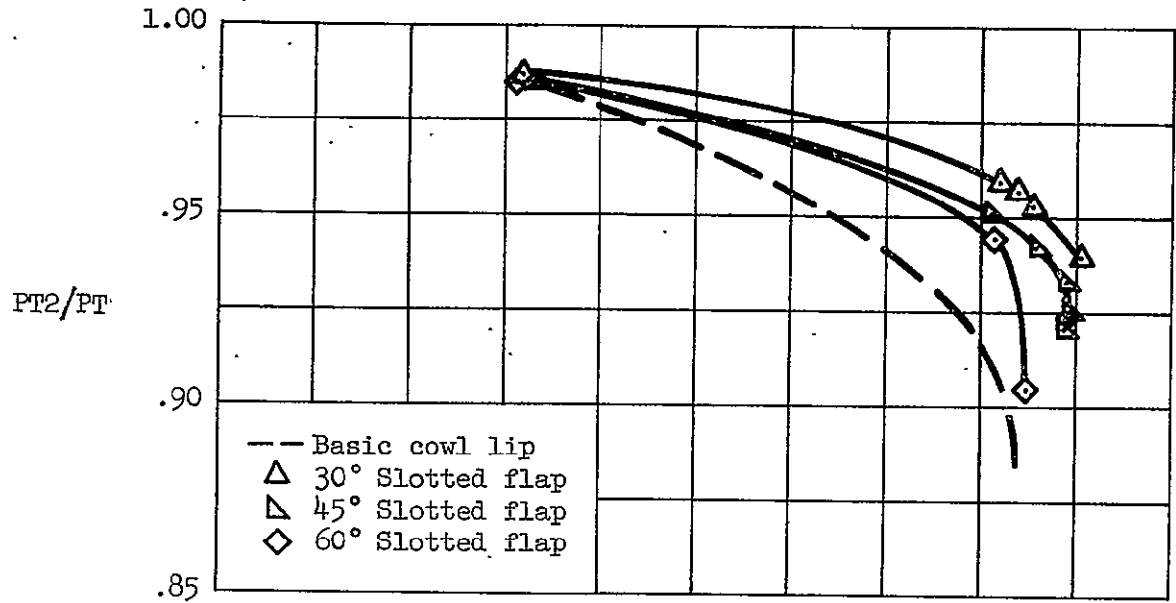
(c) $\alpha = 56^\circ$

Figure 13.- Concluded.



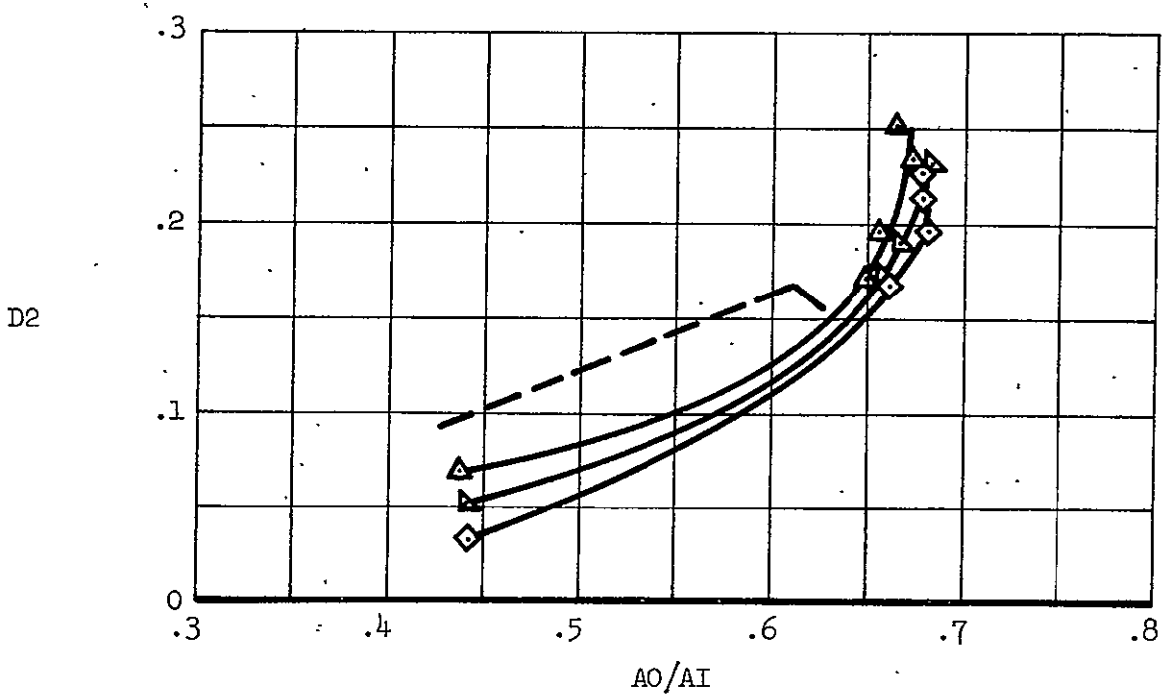
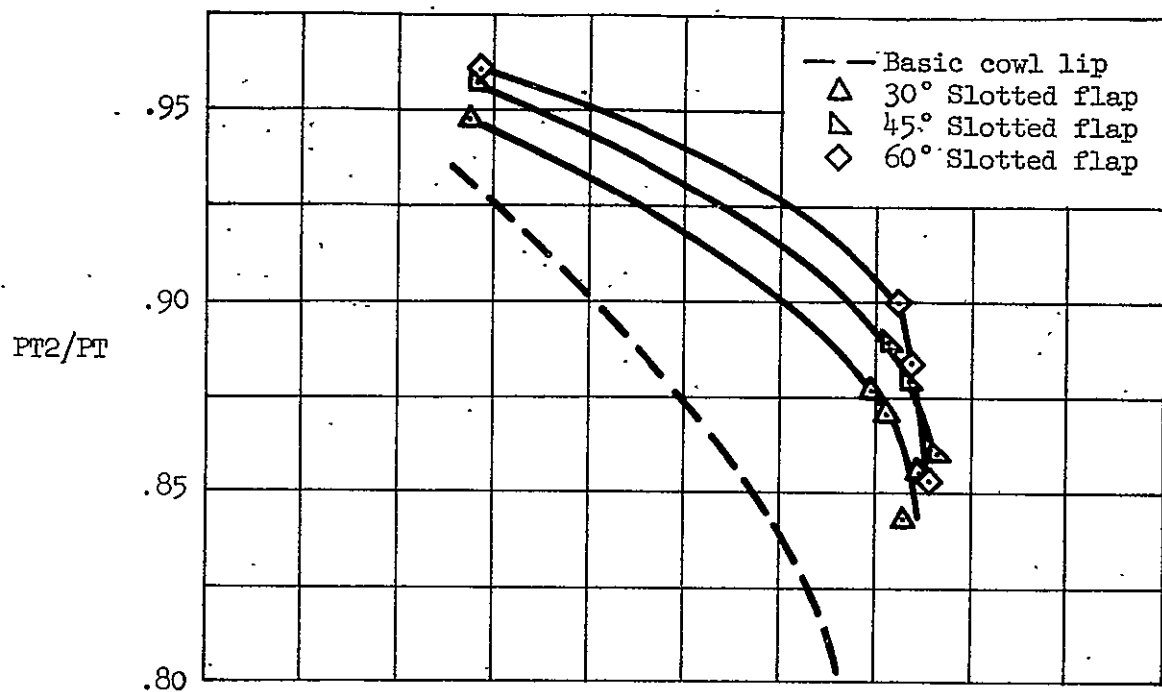
(a) $\alpha = 30^\circ$

Figure 14.- Performance of isolated inlet with slotted cowl flap; $M = 0.9$,
 $\beta = 0^\circ$.



(b) $\alpha = 40^\circ$

Figure 14.- Continued.



(c) $\alpha = 56^\circ$

Figure 14.- Concluded.

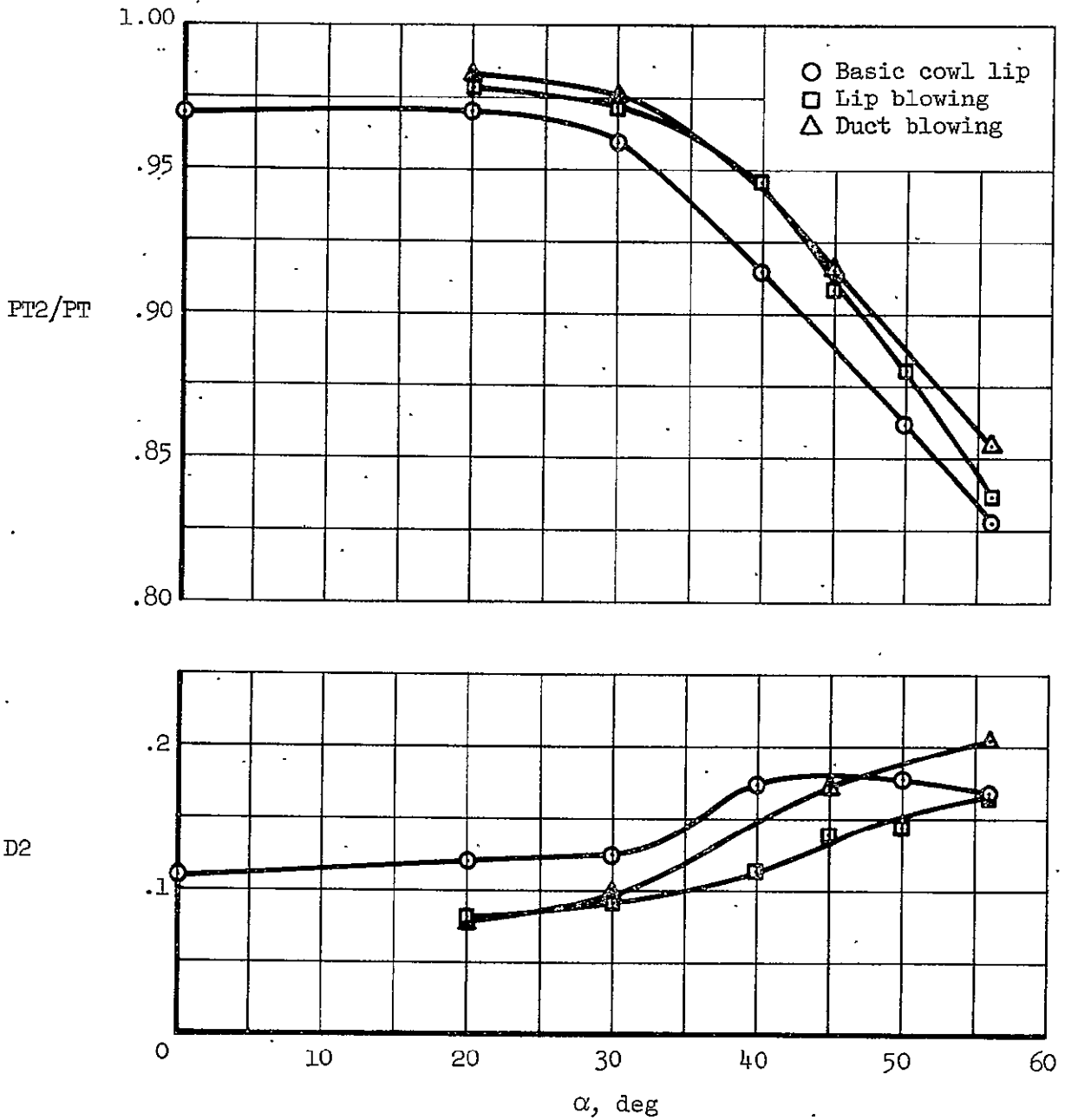
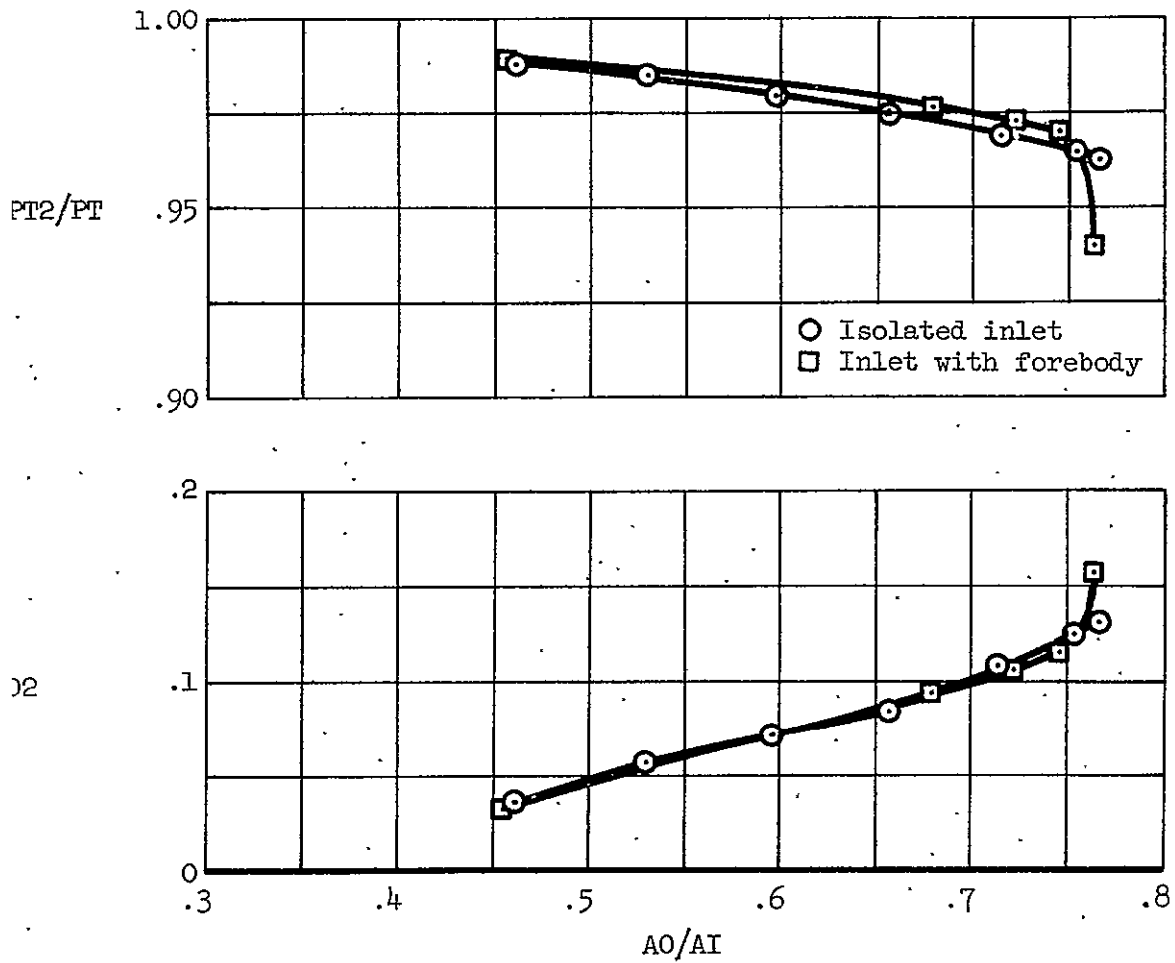
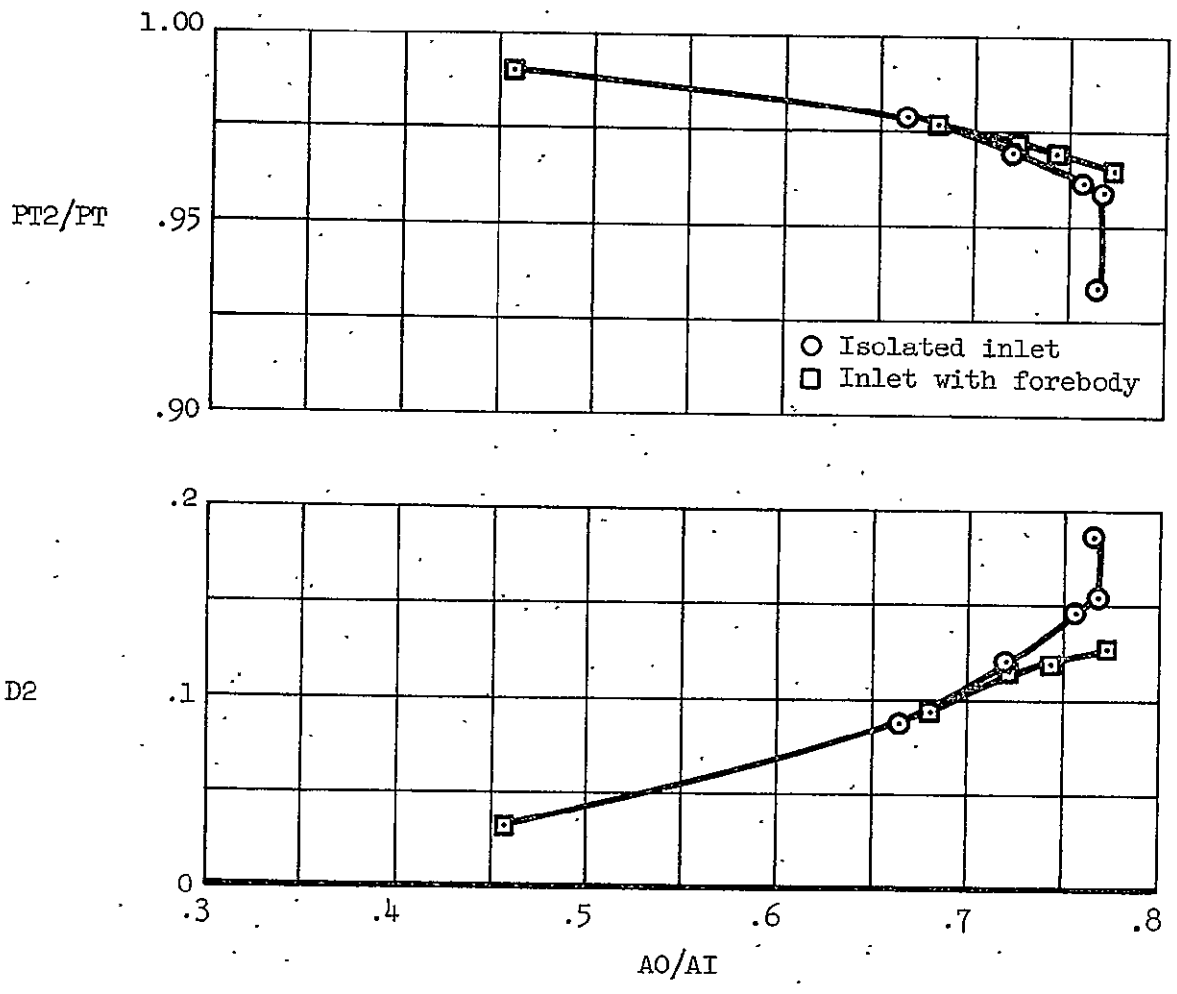


Figure 15.- Performance of isolated inlet with tangential blowing cowl slot and diffuser blowing; $M = 0.9$, $\beta = 0^\circ$.



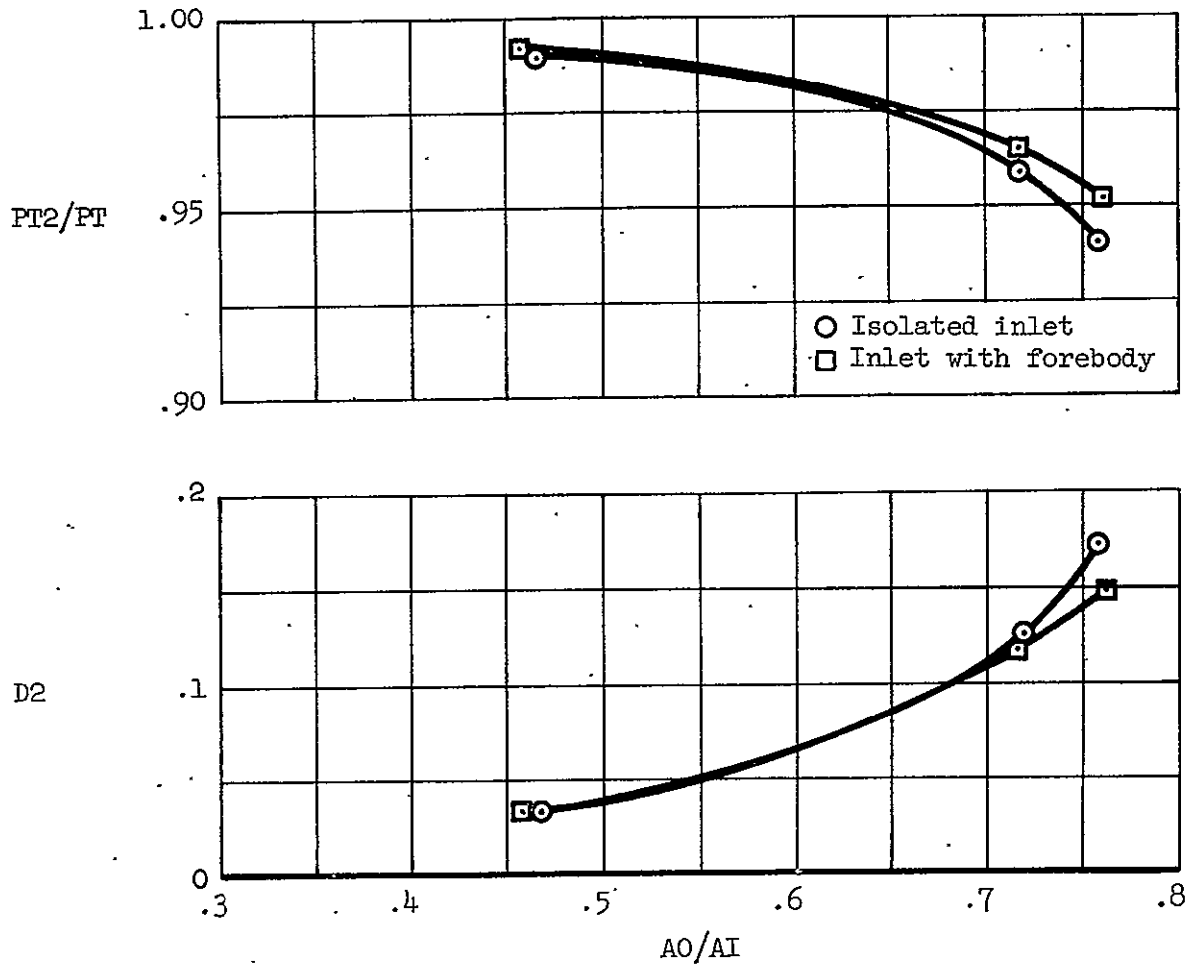
(a) $\alpha = 0^\circ$

Figure 16.- Performance of inlet with basic cowl lip and forebody; $M = 0.9$, $\beta = 0^\circ$.



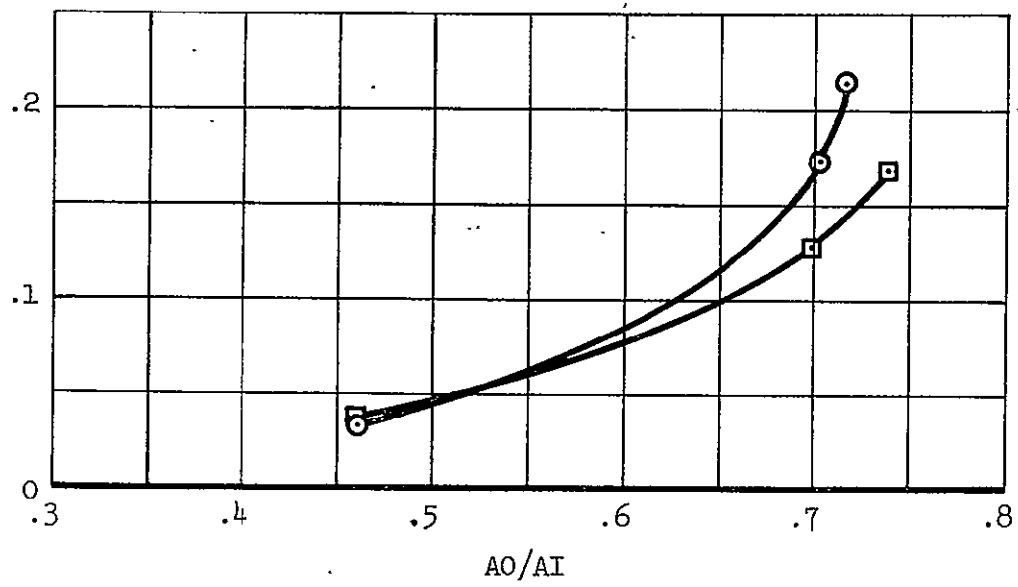
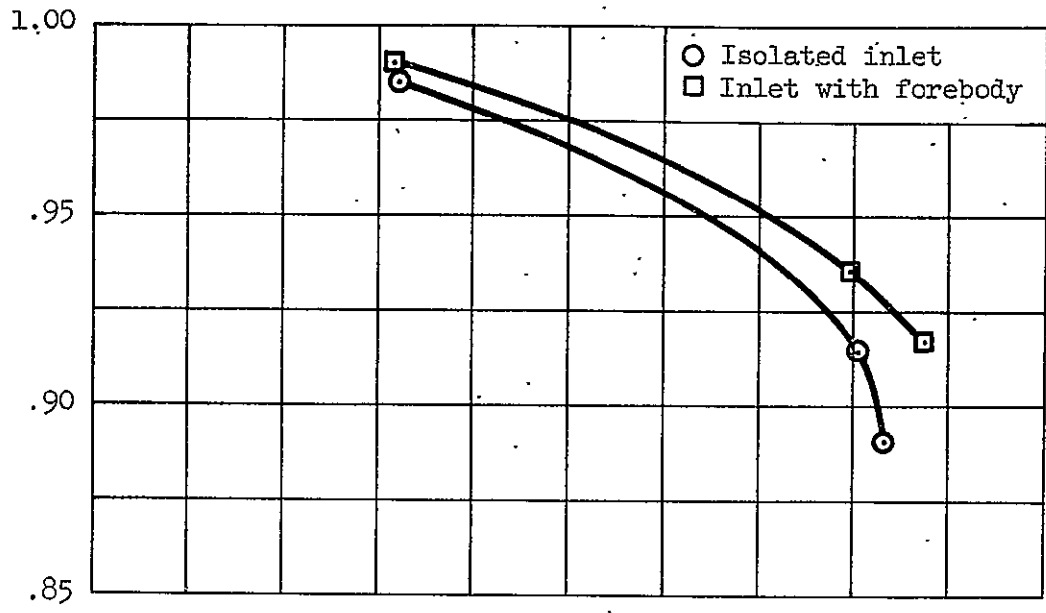
(b) $\alpha = 20^\circ$

Figure 16.- Continued.



(c) $\alpha = 30^\circ$

Figure 16.- Continued.



(d) $\alpha = 40^\circ$

Figure 16.- Concluded.

APPENDIX
SAMPLE OF TABULATED DATA

TST-161 PH-1 TN-14 17:93

IO-PRESSOUT1

03 MAY 76@18:56

RUN:SEQ
17:93

CONF	MACH	Q	PT	P	TTR	TR	RN/FT	ALPHA	BETA	PREF	WC2	PT2/PT	AO/AI	D2	PTRMS	MTH	FLAP/SLAT
1	0.901	712.7	2125	1255	574.8	494.6	4.031	0.28	0.11	1418	244.0	0.9629	0.7660	0.1305	0.0000	0.856	0

GX1	DX1	DX2	KA2	KC2	KRA2	PERCENT	WC2	QI/PT2	KTHETA	DS	KTHETAS
0.0000	0.2735	0.0520	0.1914	0.0765	0.1893	112.4	0.1884	0.0517	36.48	0.0517	

(AN/NSQRPT)MAX	RING1	RING2	RING3	RING4	RING5	THETA	RING1	RING2	RING3	RING4	RING5
	0.0039	0.0097	0.0141	0.0113	0.0125		82.83	99.89	87.51	121.6	108.8

ID	IDCMAX	IDRMAX	IDC1	IDC2	IDC3	IDC4	IDC5	IDCHUB	IDCTIP	IDR1	IDR2	IDR3	IDR4	IDR5
0.8216	0.0391	0.0603	0.0131	0.0191	0.0262	0.0458	0.0323	0.0161	0.0391	0.0354	0.0261	0.0129	0.0141	0.0603

PA1/P	PA1/PDX	WA1/W2	CMU10	CMU11	VIA10	VIA11	PA2/P	PA2/PDY	WA2/W2	CMU20	CMU21	VIA20	VIA21	(WA1+WA2)/W2	CMU0	CMU1
0.0000	0.0000	0.0000	0.0000	0.0000	0.0000	0.0000	0.0000	0.0000	0.0000	0.0000	0.0000	0.0000	0.0000	0.0000	0.0000	0.0000

(PT2R/PT2)BASE	RING1	RING2	RING3	RING4	RING5	(PT2R/PT2)MEAS	RING1	RING2	RING3	RING4	RING5
	1.075	1.054	1.036	0.9373	0.8978		1.035	1.026	1.013	0.9859	0.9397

A MINUS SIGN INDICATES A BAD COMPRESSOR FACE PRESSURE

CF101	CF102	CF103	CF104	CF105	CF106	CF107	CF108	CF201	CF202	CF203	CF204	CF205	CF206	CF207	CF208
0.9989	0.9992	0.9844	0.9974	0.9994	0.9989	0.9988	0.9990	0.9936	0.9982	0.9896	0.9883	0.9915	0.9753	0.9695	0.9977
CF301	CF302	CF303	CF304	CF305	CF306	CF307	CF308	CF401	CF402	CF403	CF404	CF405	CF406	CF407	CF408
0.9898	0.9780	0.9615	0.9824	0.9501	0.9646	0.9891	0.9868	0.9514	0.9325	0.9666	0.9541	0.9051	0.9425	0.9952	0.9464
CF501	CF502	CF503	CF504	CF505	CF506	CF507	CF508	PT1	SPF1	SPF2	SPF3	SPF4			
0.9151	0.8956	0.9305	0.8953	0.8737	0.8898	0.9377	0.9010								

R101	R102	R103	R104	R105	R106	R201	R202	R203	R204	R205	R206	R207	R208	
0.9993	0.9993	0.9993	0.9994	0.9983	0.9993	0.9954	0.9993	0.9995	0.9991	0.9985	0.9985	0.9985	0.9988	
R301	R302	R303	R304	R305	R306	R307	R308	R309	R310	R401	R402	R403	R404	R405
0.8866	0.9254	0.9248	0.9935	0.9991	0.9991	0.9992	0.9994	0.9988	0.9992	0.9202	0.9990	0.9976	0.9986	0.9985
R406	R407	R408	R409	R410	R501	R502	R503	R504	R505	R506	R507	R508	R509	R510
0.9992	0.9993	0.9996	0.9991	0.9992	0.8420	0.8646	0.9027	0.9435	0.9786	0.9986	0.9991	0.9986		0.9993

P301	P302	P303	P304	P305	P306	P307	P308	P3/PT2	PD101	PD102	PD103	PD104	PD105	PD106	PD107	
0.5701	0.5774	0.5809	0.5703	0.5678	0.5411	0.5567	0.5800	0.5899	0.6815	0.6745	0.6097	0.5706	0.6147	0.6883	0.7232	
PD108	PD109	PD110	PD111	PD201	PD202	PD203	PD204	PD205	PD206	PD207	PD208	PD209	PD210	PD211	PD212	PD213
0.7446	0.7686	0.8138	0.8219	0.7200	0.6621	0.6797	0.6540	0.6932	0.7248	0.6799	0.7185	0.7240	0.7394	0.7456	0.7840	0.8121

TST-161 PH-1 TN-14 17:94

ID-PRESSOUT1

03 MAY 76@18:56

RUN:SEQ
17:94

CONF	MACH	Q	PT	P	TTR	TR	RN/FT	ALPHA	BETA	PREF	WC2	PT2/PT	AO/AI	D2	PT RMS	MTH	FLAP/SLAT
1	0.901	713.1	2125	1255	574.7	494.5	4.032	0.28	0.13	1418	226.0	0.9689	0.7138	0.1086	0.0000	0.723	0

GX1	DX1	DX2	KA2	KC2	KRA2	PERCENT	WC2	QI/PT2	KTHETA	DS	KTHETAS
0.0000	0.6551	0.0222	0.5316	0.0326	0.2441	104.1	0.1611	0.0343	28.38	0.0305	

(AN/NSQRPT)MAX	RING1	RING2	RING3	RING4	RING5	THETA	RING1	RING2	RING3	RING4	RING5
	0.0033	0.0044	0.0076	0.0074	0.0061		86.35	168.4	101.6	0.0000	0.0000

ID	IDCMAX	IDRMAX	IDC1	IDC2	IDC3	IDC4	IDC5	IDCHUB	IDCTIP	IDR1	IDR2	IDR3	IDR4	IDR5
0.6522	0.0248	0.0504	0.0098	0.0061	0.0233	0.0230	0.0266	0.0080	0.0248	0.0296	0.0232	0.0112	0.0137	0.0504

PA1/P	PA1/PDX	WA1/W2	CMU10	CMU11	VIA10	VIA11	PA2/P	PA2/PDY	WA2/W2	CMU20	CMU21	VIA20	VIA21	(WA1+WA2)/W2	CMU0	CMUL
0.0000	0.0000	0.0000	0.0000	0.0000	0.0000	0.0000	0.0000	0.0000	0.0000	0.0000	0.0000	0.0000	0.0000	0.0000	0.0000	0.0000

(PT2R/PT2)BASE	RING1	RING2	RING3	RING4	RING5	(PT2R/PT2)MEAS	RING1	RING2	RING3	RING4	RING5
	1.074	1.054	1.036	0.9385	0.8980		1.030	1.023	1.011	0.9863	0.9496

A MINUS SIGN INDICATES A BAD COMPRESSOR FACE PRESSURE

CF101	CF102	CF103	CF104	CF105	CF106	CF107	CF108	CF201	CF202	CF203	CF204	CF205	CF206	CF207	CF208
0.9996	0.9993	0.9880	0.9970	0.9987	0.9992	0.9995	0.9993	-0.9861	0.9977	0.9981	-0.9894	0.9911	0.9858	0.9855	0.9977
CF301	CF302	CF303	CF304	CF305	CF306	CF307	CF308	CF401	CF402	CF403	CF404	CF405	CF406	CF407	CF408
0.9762	0.9815	0.9906	0.9841	0.9571	0.9731	0.9851	0.9903	0.9334	0.9426	0.9762	0.9648	0.9231	0.9537	0.9960	0.9556
CF501	CF502	CF503	CF504	CF505	CF506	CF507	CF508	PT1	SPF1	SPF2	SPF3	SPF4			
0.9084	0.9100	0.9519	0.9126	0.8944	0.9145	0.9481	0.9211								

R101	R102	R103	R104	R105	R106	R201	R202	R203	R204	R205	R206	R207	R208
0.9992	0.9994	0.9993	0.9996	0.9988	0.9992	0.9964	0.9993	0.9998	0.9993	0.9987	0.9996	0.9992	0.9987
R301	R302	R303	R304	R305	R306	R307	R308	R309	R310	R401	R402	R403	R404
0.9225	0.9504	0.9556	0.9976	0.9992	0.9994	0.9992	0.9998	0.9991	0.9990	0.9728	0.9994	0.9985	0.9993
R406	R407	R408	R409	R410	R501	R502	R503	R504	R505	R506	R507	R508	R509
0.9995	0.9995	0.9997	0.9993	0.9995	0.8716	0.8897	0.9206	0.9582	0.9888	0.9992	0.9992	0.9986	0.9995

P301	P302	P303	P304	P305	P306	P307	P308	P3/PT2	PD101	PD102	PD103	PD104	PD105	PD106	PD107
0.5870	0.6054	0.6094	0.5950	0.5946	0.5658	0.5857	0.6067	0.6127	0.6918	0.7182	0.6838	0.6688	0.6940	0.7455	0.7719
PD108	PD109	PD110	PD111	PD201	PD202	PD203	PD204	PD205	PD206	PD207	PD208	PD209	PD210	PD211	PD212
0.7891	0.8064	0.8435	0.8488	0.7772	0.7359	0.7460	0.7334	0.7540	0.7808	0.7490	0.7713	0.7735	0.7831	0.7872	0.8194
															0.8413

54

TST-161 PH-1 TN-14 17:95

ID-PRESSOUT1

03 MAY 76a18:56

RUN:SEQ
17:95

CONF	MACH	Q	PT	P	TTR	TR	RN/FT	ALPHA	BETA	PREF	WC2	PT2/PT	AO/AI	D2	PTRMS	MTH	FLAP/SLAT
1	0.901	712.7	2125	1255	576.2	495.8	4.018	0.25	0.14	1417	206.4	0.9751	0.6563	0.0843	0.0000	0.617	0
GX1	DX1	DX2	KA2	KC2	KRA2	PERCENT	WC2	QI/PT2	KTHETA	DS	KTHETAS						
0.0000	0.1419	0.6175	0.1919	0.0257	0.0777	95.13	0.1324	0.0287	27.60	0.0218							
(AN/NSQRPT)MAX	RING1	RING2	RING3	RING4	RING5	THETA	RING1	RING2	RING3	RING4	RING5						
	0.0024	0.0020	0.0045	0.0061	0.0055		83.18	152.3	90.63	0.0000	0.0000						
ID	IDCMAX	IDRMAX	IDC1	IDC2	IDC3	IDC4	IDC5	IDCHUB	IDCTIP	IDR1	IDR2	IDR3	IDR4	IDR5			
0.5373	0.0234	0.0402	0.0078	0.0102	0.0195	0.0275	0.0192	0.0090	0.0234	0.0235	0.0187	0.0085	0.0104	0.0402			
PA1/P	PA1/PDX	WA1/W2	CMU10	CMU11	VIA10	VIA11	PA2/P	PA2/PDY	WA2/W2	CMU20	CMU21	VIA20	VIA21	(WA1+WA2)/W2	CMU0	CMUL	
0.0000	0.0000	0.0000	0.0000	0.0000	0.0000	0.0000	0.0000	0.0000	0.0000	0.0000	0.0000	0.0000	0.0000	0.0000	0.0000	0.0000	
(PT2R/PT2)BASE	RING1	RING2	RING3	RING4	RING5	(PT2R/PT2)MEAS	RING1	RING2	RING3	RING4	RING5						
	1.027	1.029	1.022	0.9738	0.9463		1.023	1.019	1.008	0.9896	0.9598						

A MINUS SIGN INDICATES A BAD COMPRESSOR FACE PRESSURE

CF101	CF102	CF103	CF104	CF105	CF106	CF107	CF108	CF201	CF202	CF203	CF204	CF205	CF206	CF207	CF208
0.9993	0.9993	0.9905	0.9982	0.9992	0.9992	0.9993	0.9993	-0.9834	0.9986	0.9986	-0.9925	0.9926	0.9897	0.9929	0.9983
CF301	CF302	CF303	CF304	CF305	CF306	CF307	CF308	CF401	CF402	CF403	CF404	CF405	CF406	CF407	CF408
0.9716	0.9890	0.9911	0.9886	0.9644	0.9810	0.9868	0.9946	0.9382	0.9599	0.9801	0.9723	0.9421	0.9621	0.9966	0.9689
CF501	CF502	CF503	CF504	CF505	CF506	CF507	CF508	PT1	SPF1	SPF2	SPF3	SPF4			
0.9190	0.9293	0.9618	0.9303	0.9172	0.9299	0.9617	0.9380								
R101	R102	R103	R104	R105	R106	R201	R202	R203	R204	R205	R206	R207	R208		
0.9993	0.9995	0.9994	0.9994	0.9984	0.9997	0.9979	0.9994	0.9993	0.9992	0.9990	0.9992	0.9988	0.9996		
R301	R302	R303	R304	R305	R306	R307	R308	R309	R310	R401	R402	R403	R404	R405	
0.9425	0.9668	0.9738	0.9989	0.9996	0.9996	0.9995	0.9994	0.9988	0.9993	0.9850	0.9994	0.9992	0.9990	0.9987	
R406	R407	R408	R409	R410	R501	R502	R503	R504	R505	R506	R507	R508	R509	R510	
0.9996	0.9996	0.9997	0.9991	0.9998	0.9035	0.9196	0.9465	0.9705	0.9935	0.9991	0.9988	0.9988		0.9993	
P301	P302	P303	P304	P305	P306	P307	P308	P3/PT2	PD101	PD102	PD103	PD104	PD105	PD106	PD107
0.6068	0.6313	0.6382	0.6201	0.6226	0.5934	0.6126	0.6328	0.6355	0.7095	0.7624	0.7489	0.7442	0.7625	0.7994	0.8184
PD108	PD109	PD110	PD111	PD201	PD202	PD203	PD204	PD205	PD206	PD207	PD208	PD209	PD210	PD211	PD212
0.8316	0.8450	0.8732	0.8766	0.8300	0.7975	0.8019	0.7934	0.8088	0.8291	0.8059	0.8206	0.8206	0.8268	0.8293	0.8531
															0.8721

TST-161 PH-1 TN-14 17:96

10-PRESSOUT1

03 MAY 76@18:56

RUN:SEQ
17:96

CONF	MACH	Q	PT	P.	TTR	TR	RN/FT	ALPHA	BETA	PREF	WC2	PT2/PT	AO/AI	D2	PTRMS	MTH	FLAP/SLAT
1	0.899	711.4	2124	1257	575.4	495.3	4.022	0.27	0.13	1418	186.5	0.9804	0.5963	0.0723	0.0000	0.530	0
GX1		DX1	DX2	KA2	KC2	KRA2	PERCENT	WC2	QI/PT2	KTHETA	DS	KTHETAS					
0.0000		0.1271	0.0318	0.2861	0.0467	0.1010	85.95	0.1059	0.0307	26.86	0.0221						
(AN/NSQRPT)MAX - RING1 RING2 RING3 RING4 RING5 THETA- - RING1 RING2 RING3 RING4 RING5																	
		0.0019	0.0023	0.0029	0.0057	0.0048			81.49	85.11	78.26	0.0000	0.0000				
ID	IDC	MAX	IDR	MAX	IDC1	IDC2	IDC3	IDC4	IDC5	IDCHUB	IDCTIP	IDR1	IDR2	IDR3	IDR4	IDR5	
0.4380	0.0248	0.0305	0.0063	0.0158	0.0235	0.0332	0.0164	0.0111	0.0248	0.0187	0.0140	0.0057	0.0079	0.0305			
PA1/P	PA1/PDX	WA1/W2	CMU10	CMU11	VIA10	VIA11	PA2/P	PA2/PDY	WA2/W2	CMU20	CMU21	VIA20	VIA21	(WA1+WA2)/W2	CMUO	CMUL	
0.0000	0.0000	0.0000	0.0000	0.0000	0.0000	0.0000	0.0000	0.0000	0.0000	0.0000	0.0000	0.0000	0.0000	0.0000	0.0000	0.0000	
(PT2R/PT2)BASE - RING1 RING2 RING3 RING4 RING5 (PT2R/PT2)HEAS - RING1 RING2 RING3 RING4 RING5																	
		1.022	1.025	1.021	0.9780	0.9545			1.019	1.014	1.006	0.9921	0.9695				

96

A MINUS SIGN INDICATES A BAD COMPRESSOR FACE PRESSURE

CF101	CF102	CF103	CF104	CF105	CF106	CF107	CF108	CF201	CF202	CF203	CF204	CF205	CF206	CF207	CF208
0.9992	0.9998	0.9925	0.9989	0.9997	0.9993	0.9996	1.0002	-0.9785	0.9998	0.9993	-0.9943	0.9941	0.9922	0.9950	0.9992
CF301	CF302	CF303	CF304	CF305	CF306	CF307	CF308	CF401	CF402	CF403	CF404	CF405	CF406	CF407	CF408
0.9629	0.9955	0.9929	0.9911	0.9733	0.9859	0.9897	0.9966	0.9401	0.9748	0.9857	0.9799	0.9527	0.9708	0.9973	0.9801
CF501	CF502	CF503	CF504	CF505	CF506	CF507	CF508	PT1	SPF1	SPF2	SPF3	SPF4			
0.9293	0.9493	0.9704	0.9471	0.9344	0.9450	0.9699	0.9584								
R101	R102	R103	R104	R105	R106	R201	R202	R203	R204	R205	R206	R207	R208		
0.9998	0.9999	0.9993	0.9997	0.9988	1.000	0.9984	1.000	0.9998	0.9993	0.9992	0.9999	0.9996	0.9995		
R301	R302	R303	R304	R305	R306	R307	R308	R309	R310	R401	R402	R403	R404	R405	
0.9580	0.9781	0.9864	0.9992	0.9999	0.9992	0.9996	0.9999	0.9994	0.9997	0.9892	1.000	0.9997	0.9998	0.9987	
R406	R407	R408	R409	R410	R501	R502	R503	R504	R505	R506	R507	R508	R509	R510	
1.000	0.9992	0.9998	0.9993	1.000	0.9284	0.9417	0.9659	0.9818	0.9972	0.9995	0.9993	0.9989	0.9991		
P301	P302	P303	P304	P305	P306	P307	P308	P3/PT2	PD101	PD102	PD103	PD104	PD105	PD106	PD107
0.6758	0.6559	0.6630	0.6452	0.6483	0.6175	0.6372	0.6580	0.6567	0.7281	0.8048	0.8040	0.8044	0.8195	0.8463	0.8601
PD108	PD109	PD110	PD111	PD201	PD202	PD203	PD204	PD205	PD206	PD207	PD208	PD209	PD210	PD211	PD212
0.8698	0.8798	0.9006	0.9025	0.8762	0.8486	0.8469	0.8444	0.8549	0.8711	0.8532	0.8631	0.8623	0.8663	0.8676	0.8846
0.8997															

TST-161 PH-1 TN-14 17:97

ID-PRESSOUT1

03 MAY 76 218:56

RUN:SEQ
17:97

CONF	MACH	Q	PT	P	TTR	TR	RN/FT	ALPHA	BETA	PREF	WC2	PT2/PT	AO/AI	D2	PT RMS	MTH	FLAP/SLAT		
1	0.898	710.2	2124	1259	575.1	495.3	4.022	0.27	0.14	1418	164.7	0.9846	0.5291	0.0575	0.0000	0.449	0		
GX1	DX1	DX2	KAZ	KC2	KRA2	PERCENT	WC2	QI/PT2	KTHETA	DS	KTHETAS								
0.0000	0.2622	0.0552	1.8948	0.0812	0.2276	75.91	0.0804	0.0432	26.05	0.0378									
(AN/NSQRPT)MAX - RING1 RING2 RING3 RING4 RING5 THETA- - RING1 RING2 RING3 RING4 RING5																			
										0.0014	0.0038	0.0046	0.0049	0.0039	83.76	74.47	71.31	0.0000	0.0000
ID	IDCMAX	IDRMAX	IDC1	IDC2	IDC3	IDC4	IDC5	IDCHUB	IDCTIP	IDR1	IDR2	IDR3	IDR4	IDR5					
0.3399	0.0245	0.0215	0.0042	0.0207	0.0334	0.0361	0.0128	0.0124	0.0245-0.0147-0.0095-0.0024	0.0051	0.0215								
PA1/P	PA1/PDX	WA1/W2	CMU10	CMU11	VIA10	VIA11	PA2/P	PA2/PDY	WA2/W2	CMU20	CMU21	VIA20	VIA21	{WA1+WA2}/W2	CMU0	CMUL			
0.0000	0.0000	0.0000	0.0000	0.0000	0.0000	0.0000	0.0000	0.0000	0.0000	0.0000	0.0000	0.0000	0.0000	0.0000	0.0000	0.0000			
(PT2R/PT2)BASE - RING1 RING2 RING3 RING4 RING5 (PT2R/PT2)MEAS - RING1 RING2 RING3 RING4 RING5																			
										0.9863	0.9960	1.009	1.009	1.002	1.015	1.010	1.002	0.9949	0.9785

A MINUS SIGN INDICATES A BAD COMPRESSOR FACE PRESSURE

CF101	CF102	CF103	CF104	CF105	CF106	CF107	CF108	CF201	CF202	CF203	CF204	CF205	CF206	CF207	CF208	
0.9994	0.9995	0.9949	0.9993	0.9996	0.9999	1.0000	0.9997-0.9736	0.9996	0.9992-0.9954	0.9946	0.9939	0.9971	0.9985			
CF301	CF302	CF303	CF304	CF305	CF306	CF307	CF308	CF401	CF402	CF403	CF404	CF405	CF406	CF407	CF408	
0.9541	0.9978	0.9943	0.9929	0.9795	0.9893	0.9918	0.9960	0.9440	0.9861	0.9893	0.9857	0.9651	0.9790	0.9976	0.9898	
CF501	CF502	CF503	CF504	CF505	CF506	CF507	CF508	PT1	SPF1	SPF2	SPF3	SPF4				
0.9433	0.9670	0.9787	0.9587	0.9508	0.9591	0.9775	0.9723									
R101	R102	R103	R104	R105	R106	R201	R202	R203	R204	P205	R206	R207	R208			
0.9997	0.9998	0.9999	0.9998	0.9993	0.9997	0.9990	0.9999	0.9999	0.9997	0.9996	0.9996	0.9994	0.9994			
K301	R302	R303	R304	R305	R306	R307	R308	R309	R310	R401	R402	R403	R404	R405		
0.9701	0.9842	0.9894	0.9993	0.9995	0.9995	0.9998	0.9993	0.9997	0.9996	0.9935	0.9999	0.9993	0.9996	0.9988		
R406	R407	R408	R409	R410	R501	R502	R503	R504	R505	R506	R507	R508	R509	R510		
0.9999	0.9996	0.9998	1.000	0.9997	0.9476	0.9596	0.9779	0.9879	0.9980	0.9993	0.9998	0.9989	0.9999			
P301	P302	P303	P304	P305	P306	P307	P308	P3/PT2	PD101	PD102	PD103	PD104	PD105	PD106	PD107	
0.6471	0.6804	0.6885	0.6708	0.6730	0.6424	0.6645	0.6843	0.6793	0.7482	0.8428	0.8503	0.8556	0.8674	0.8867	0.8964	
PD108	PD109	PD110	PD111	PD201	PD202	PD203	PD204	PD205	PD206	PD207	PD208	PD209	PD210	PD211	PD212	PD213
0.9032	0.9094	0.9243	0.9265	0.9142	0.8911	0.8894	0.8884	0.8941	0.9063	0.8925	0.8992	0.8974	0.9001	0.9017	0.9126	0.9241

TST-161 PH-1 TN-14 17:98

ID-PRESSOUT1

03 MAY 76 18:56

RUN:SEQ
17:98

CONF	MACH	Q	PT	P	TTR	TR	RN/FT	ALPHA	BETA	PREF	WC2	PT2/PT	AO/AI	D2	PTRMS	MTH	FLAP	SLAT
1	0.900	712.3	2125	1256	577.1	496.6	4.009	0.29	0.15	1417	142.7	0.9883	0.4598	0.0355	0.0000	0.377	0	

GX1	DX1	DX2	KA2	KC2	KRA2	PERCENT	WC2	QI/PT2	KTHETA	DS	KTHETAS
0.0000	0.6951	0.1013	5.8106	0.1489	0.2919	65.76	0.0588	0.0718	25.20	0.0805	

(AN/NSQRPT)MAX	RING1	RING2	RING3	RING4	RING5	THETA	RING1	RING2	RING3	RING4	RING5
	0.0037	0.0061	0.0037	0.0028	0.0044		91.96	97.34	0.0000	0.0000	0.0000

ID	IDCMAX	IDRMAX	IDC1	IDC2	IDC3	IDC4	IDC5	IDCHUB	IDCTIP	IDR1	IDR2	IDR3	IDR4	IDR5
0.2025	0.0123	0.0138	0.0088	0.0157	0.0206	0.0120	0.0104	0.0123	0.0112	0.0088	0.0051	0.0015	0.0017	0.0138

PA1/P	PA1/PDX	WA1/W2	CMU10	CMU11	VIA10	VIA11	PA2/P	PA2/PDY	WA2/W2	CMU20	CMU21	VIA20	VIA21	(WA1+WA2)/W2	CMU0	CMU1
0.0000	0.0000	0.0000	0.0000	0.0000	0.0000	0.0000	0.0000	0.0000	0.0000	0.0000	0.0000	0.0000	0.0000	0.0000	0.0000	0.0000

(PT2R/PT2)BASE	RING1	RING2	RING3	RING4	RING5	(PT2R/PT2)MEAS	RING1	RING2	RING3	RING4	RING5
	0.9824	0.9924	1.011	1.010	1.006		1.009	1.005	1.002	0.9983	0.9862

A MINUS SIGN INDICATES A BAD COMPRESSOR FACE PRESSURE

CF101	CF102	CF103	CF104	CF105	CF106	CF107	CF108	CF201	CF202	CF203	CF204	CF205	CF206	CF207	CF208
0.9882	0.9979	0.9969	0.9993	0.9993	0.9991	0.9994	0.9955	-0.9778	0.9955	0.9987	-0.9961	0.9959	0.9961	0.9976	0.9889
0.9694	0.9970	0.9945	0.9940	0.9850	0.9925	0.9936	0.9920	0.9700	0.9925	0.9919	0.9890	0.9747	0.9839	0.9976	0.9931
0.9677	0.9783	0.9837	0.9692	0.9644	0.9691	0.9848	0.9800		PT1	SPF1	SPF2	SPF3	SPF4		

R101	R102	R103	R104	R105	R106	R201	R202	R203	R204	R205	R206	R207	R208
0.9991	0.9989	0.9996	0.9991	0.9988	0.9992	0.9986	0.9992	0.9993	0.9991	0.9994	0.9993	0.9990	0.9988
0.9789	0.9884	0.9907	0.9996	0.9987	0.9996	0.9995	0.9994	0.9993	0.9991	0.9957	0.9996	0.9995	0.9992
0.9986	0.9993	0.9991	0.9992	0.9993	0.9641	0.9731	0.9859	0.9914	0.9988	1.0000	0.9989	0.9987	0.9992

P301	P302	P303	P304	P305	P306	P307	P308	P3/PT2	PD101	PD102	PD103	PD104	PD105	PD106	PD107
0.6687	0.7049	0.7139	0.6959	0.6963	0.6664	0.6879	0.7080	0.7010	0.7689	0.8758	0.8886	0.8958	0.9054	0.9188	0.9249
0.9295	0.9337	0.9438	0.9468	0.9431	0.9239	0.9217	0.9206	0.9244	0.9329	0.9225	0.9272	0.9257	0.9270	0.9280	0.9359
															0.9447

58

IST-161 PH-1 TN-14 17:99

ID-PRESSOUT1

03 MAY 76 18:56

RUN:SEQ

17:59

CONF	MACH	Q	PT	P	TTR	TR	RN/FT	ALPHA	BETA	PREF	WC2	PT2/PT	AO/AI	D2	PTMS	MTH	FLAP/SLAT
1	0.902	713.8	2124	1253	576.9	496.1	4.013	0.27	0.14	1417	239.5	0.9650	0.7532	0.1248	0.0000	0.817	0
GX1	DX1	DX2	KA2	KC2	KRA2	PERCENT	WC2	Q1/PT2	KTHETA	DS	KTHETAS						
0.0000	0.2753	0.0426	0.1927	0.0627	0.2008	110.4	0.1817	0.0445	32.28	0.0413							
(AN/NSQRPT)MAX - RING1 RING2 RING3 RING4 RING5 THETA - RING1 RING2 RING3 RING4 RING5																	
0.0037 0.0080 0.0111 0.0086 0.0112 84.92 93.99 93.18 118.7 0.0000																	
ID	IDCMAX	IDRMAX	IDC1	IDC2	IDC3	IDC4	IDC5	IDCHUB	IDCTIP	IDR1	IDR2	IDR3	IDR4	IDR5			
0.7768	0.0367	0.0571	0.0116	0.0162	0.0241	0.0418	0.0316	0.0139	0.0367	0.0338	0.0258	0.0128	0.0153	0.0571			
PA1/P	PA1/PDX	WA1/W2	CMU10	CMU11	VIA10	VIA11	PA2/P	PA2/PDY	WA2/W2	CMU20	CMU21	VIA20	VIA21	(WA1+WA2)/W2	CMU0	CMU1	
0.0000	0.0000	0.0000	0.0000	0.0000	0.0000	0.0000	0.0000	0.0000	0.0000	0.0000	0.0000	0.0000	0.0000	0.0000	0.0000	0.0000	
(PT2R/PT2)BASE - RING1 RING2 RING3 RING4 RING5 (PT2R/PT2)MEAS - RING1 RING2 RING3 RING4 RING5																	
1.075 1.054 1.036 0.9373 0.8978 1.034 1.026 1.013 0.9847 0.9429																	

A MINUS SIGN INDICATES A BAD COMPRESSOR FACE PRESSURE

CF101	CF102	CF103	CF104	CF105	CF106	CF107	CF108	CF201	CF202	CF203	CF204	CF205	CF206	CF207	CF208	
0.9993	0.9999	0.9865	0.9971	0.9995	0.9996	0.9996	0.9998	0.9916	0.9980	0.9953	0.9883	0.9927	0.9808	0.9743	0.9982	
CF301	CF302	CF303	CF304	CF305	CF306	CF307	CF308	CF401	CF402	CF403	CF404	CF405	CF406	CF407	CF408	
0.9860	0.9790	0.9732	0.9821	0.9540	0.9690	0.9877	0.9877	0.9446	0.9335	0.9686	0.9571	0.9099	0.9450	0.9952	0.9477	
CF501	CF502	CF503	CF504	CF505	CF506	CF507	CF508	PT1	SPF1	SPF2	SPF3	SPF4				
0.9135	0.8987	0.9388	0.9004	0.8795	0.8954	0.9420	0.9111									
R101	R102	R103	R104	R105	R106	R201	R202	R203	R204	R205	R206	R207	R208			
0.9996	0.9994	0.9997	0.9996	0.9986	0.9997	0.9969	0.9998	0.9994	0.9998	0.9989	0.9992	0.9987	0.9992			
R301	R302	R303	R304	R305	R306	R307	R308	R309	R310	R401	R402	R403	R404	R405		
0.8979	0.9332	0.9342	0.9945	0.9994	0.9992	0.9992	0.9994	0.9995	0.9992	0.9305	0.9989	0.9985	0.9993	0.9986		
R406	R407	R408	R409	R410	R501	R502	R503	R504	R505	R506	R507	R508	R509	R510		
0.9997	0.9989	0.9991	0.9996	0.9991	0.8611	0.8709	0.9048	0.9726	0.9827	0.9992	0.9996	0.9990	0.9991			
P301	P302	P303	P304	P305	P306	P307	P308	P3/PT2	PD101	PD102	PD103	PD104	PD105	PD106	PD107	
0.5737	0.5849	0.5884	0.5766	0.5753	0.5479	0.5647	0.5868	0.5956	0.6835	0.6851	0.6307	0.6010	0.6374	0.7043	0.7359	
PD108	PD109	PD110	PD111	PD201	PD202	PD203	PD204	PD205	PD206	PD207	PD208	PD209	PD210	PD211	PD212	PD213
0.7572	0.7782	0.8214	0.8291	0.7345	0.6826	0.6982	0.6781	0.7097	0.7401	0.7000	0.7330	0.7375	0.7519	0.7566	0.7939	0.8193